

# COMBINATORICS OF TABLEAUX — GRAPHICAL REPRESENTATION OF INSERTION ALGORITHMS

DALE R. WORLEY

ABSTRACT. Many algorithms for inserting elements into tableaux are known, starting with the Robinson-Schensted algorithm. Much of those processes can be incorporated into the general framework of Fomin’s “growth diagrams”. Even for single types of tableaux, there are various alternative insertion algorithms and, due to the varying ways they are described, the relationships between the algorithms can be obscure. The distinguishing features of many algorithms can be codified into graphic “insertion diagrams” which make important aspects of the algorithms immediately apparent. We use insertion diagrams to build a graphic catalog or picture book of many of the tableau insertion algorithms in the literature.

## LIST OF FIGURES

1	The points of the quadrant $\mathbb{Q} = \mathbb{P}^2$	4
2	The points of the quadrant $\mathbb{Q}$ without coordinates	4
3	Young diagrams	4
4	Young’s lattice $\mathbb{Y}$ of partitions	5
5	Hasse diagram of the quadrant $\mathbb{Q}$	5
6	The Young graph $\mathbb{Y}$ with edges labeled with their weights/multiplicities	6
7	Young tableaux	6
8	A skeleton growth diagram	7
9	A cell extracted from the growth diagram	7
10	Conventional labels of the components of a cell	8
11	Example growth process for the permutation $(2, 3, 4, 1)$	9
12	$P$ and $Q$ tableaux generated by the example growth process	10
13	Example growth process for the permutation $(4, 1, 2, 3)$	11
14	The shape $(5, 3, 3, 1)$ with its maximal and cominimal points	12
15	Generic insertion diagram for Robinson-Schensted (row) insertion	12
16	Cells representing insertion and bumping	12
17	Generic insertion diagram for column insertion into unshifted tableaux	13
18	Generic insertion diagram for left-right insertion	14

*Date:* Jun 18, 2023.

The author would like to credit Linux, Emacs, TeX, L<sup>A</sup>T<sub>E</sub>X, AMS-L<sup>A</sup>T<sub>E</sub>X, TikZ, tikzcd, and ytableau for typesetting this paper.

The author would like to thank arXiv, Sci-Hub, Internet Archive, and Google Scholar for providing a world-class research library. Calvin Mooers predicted this situation in [Mooers1959]:

In my discussion I shall bypass treating such useful and imminent tasks as the use of machines to store, transfer, and emit texts, so that at the time that you need to refer to a paper, even in an obscure journal, you can have a copy in hand within, say, twenty-four hours. [...] Neither shall I consider the application of machines to the integration of national and international library systems so that at any first-rate library, you will have at your command the catalogs of the major collections of the world. These are all coming—but it should be noted with respect to them that the problems of human cooperation ranging from person-to-person to nation-to-nation cooperation are more serious than some of the machine and technical problems involved.

19	Growth for left-right insertion	15
20	Generic insertion diagram for McLarnan's fairy insertion	15
21	Growth for McLarnan's fairy insertion	16
22	Generic insertion diagram for the "jitter" insertion	16
23	Growth for the permutation $(1, 2, 3, 4)$ for the "jitter" algorithm	17
24	Growth for the permutation $(4, 3, 2, 1)$ for the "jitter" algorithm	17
25	Growth for the permutation $(1^\circ, 2^\circ, 3^\circ, 4^\circ)$ for the "jitter" algorithm	18
26	Growth for the permutation $(4^\circ, 3^\circ, 2^\circ, 1^\circ)$ for the "jitter" algorithm	18
27	The points of the octant $\mathbb{O}$ with and without coordinates	18
28	Shifted Young tableaux	19
29	The Hasse diagram of the octant $\mathbb{O}$	19
30	The lattice of strict partitions $\mathbb{SY}$	19
31	Generic insertion diagrams for Sagan's first algorithm	20
32	Growth for the permutation $(1, 2, 5, 4, 3)$ for Sagan's first algorithm	21
33	Generic insertion diagrams for the second shifted algorithm	21
34	Growth for the permutation $(1, 2, 5, 4, 3)$ for the second shifted algorithm	22
35	Generic insertion diagram for mixed insertion.	23
36	Growth for mixed insertion	24
37	Generic insertion diagram for double-circle insertion	25
38	Growth for double-circle insertion	26
39	Generic insertion diagrams for shifted mixed insertion	27
40	Growth for the permutation $(1, 2, 5, 4, 3)$ for the shifted mixed insertion	27
41	Generic insertion diagrams for shifted colun insertion	28
42	Growth for the permutation for McLarnan's shifted colun insertion	28
43	Growth for the permutation for McLarnan's shifted colun insertion	29
44	Generic insertion diagram for dual shifted column insertion	29
45	Growth for the permutation $(1, 3, 4, 2)$ for dual shifted column insertion	30

## 1. INTRODUCTION

Many algorithms are known for inserting elements into Young tableaux, starting with the Robinson-Schensted algorithm [Schen1961]. The algorithm has been extended in various ways. The most significant extension is Knuth's version, which allows multiple equal elements to be inserted into a tableau. However we will not be pursuing that extension in this paper.

The type of tableau involved can be changed to shifted Young tableaux (which we will examine in detail), or the more complex "oscillating tableaux" (which we will not examine). These algorithms can be incorporated into the general framework of "growth diagrams" 2.7, created by Fomin [Fom1994, Fom1995].

In all of these situations, multiple algorithms can be constructed which serve the same or very similar enumerative purposes, and often no one algorithm seems to be "natural". Due to their complexity and the varying ways they are described, the relationships between the algorithms can be obscure. For many algorithms, the distinguishing features can be codified into graphic "insertion diagrams" 4 which make important aspects of the algorithms immediately apparent. We use insertion diagrams to build a graphic catalog or picture book of many of the tableau insertion algorithms in the literature.

The concept of a “generic” insertion algorithm, an algorithm that by the choice of parameters (such as our insertion diagrams) generates a family of insertion algorithms, was pioneered by [McLar1986],<sup>1</sup> a fact I discovered after this paper was well underway.<sup>2</sup>

The power of insertion diagrams as a method of describing insertion algorithms is shown by two algorithms we introduce here, “jitter” insertion 5.5 and double-circle insertion 7.2, which we define not because they are valuable, but because insertion diagrams make easy defining algorithms with specific properties.

We introduce the extension of “biweighting” 7, factoring the weight function that is applied to the edges of the “descending” graph in Fomin’s dual graded graph construction 2.4 into two weight functions, one applied to the edges of the “ascending” graph and one to the edges of the “descending” graph. This is a small change, but it allows insertion algorithms that apply “circling” to the  $P$  tableau to be described with growth processes.

We include a discussion of McLarnan’s underappreciated “shifted column insertion” algorithm. 7.4 It is biweighted and nearly inversion self-dual.

## 2. BACKGROUND

The machinery underlying tableau insertion algorithms is defined in many works (e.g. [Fom1994, Fom1995], [Haim1989], [Roby1991]). This exposition will specialize the machinery for the situations we will be considering; applying known generalizations to this exposition is in most cases straightforward. A whirlwind summary follows.

**2.1. Basics.** We use  $\mathbb{P}$  for  $\{1, 2, 3, \dots\}$  and  $\mathbb{N}$  for  $\{0, 1, 2, \dots\}$ . We use  $[n]$  for  $\{1, 2, 3, \dots, n\}$ .

We use  $\uplus$  to denote generally joining two structures that are assumed to be disjoint. One use is the union of two disjoint sets. Other uses are for the appropriate “direct sum” of two structures of the same type. In some cases, we abuse the notation by implicitly labeling the elements of the two structures with 1 or 2 (resp.) to make the structures disjoint before taking their direct sum.

If a set  $Y$  is the set  $X$  plus one additional element, we use  $Y - X$  to denote that element. Hence  $(X \uplus \{y\}) - X = y$ .

In a poset, we use  $p \succ q$  to mean that  $p$  covers  $q$ , that is,  $p > q$  and there is no  $r$  such that  $p > r > q$ . We use  $p \triangleleft q$  to mean that  $p$  is covered by  $q$ , that is,  $q \succ p$ .

A poset  $P$  is *finitary* if every principal order ideal of  $P$  is finite.[Stan2012, sec. 3.4] A poset  $P$  has *finite covers* if for every  $p \in P$ ,  $\{q \in P : p \succ q\}$  and  $\{q \in P : p \triangleleft q\}$  are both finite. A finitary poset has finite covers downward but may not have finite covers upward.

A finitary poset is locally finite. Intuitively, a finitary poset is “finite downward” but may be “infinite upward”. Intuitively, a poset with finite covers is “finite sideways”.

**Proposition 2.1.** *If a poset  $P$  has finite covers, the following are equivalent:*

- (1)  $P$  is finitary.
- (2)  $P$  has no infinite descending chain (there does not exist  $p_1, p_2, p_3, \dots \in P$  such that  $p_1 \succ p_2 \succ p_3 \succ \dots$ ), and  $P$  has no bounded infinite ascending chain (there does not exist  $p_1, p_2, p_3, \dots, q \in P$  such that  $p_1 \triangleleft p_2 \triangleleft p_3 \triangleleft \dots \triangleleft q$ ).

*Proof.* (1)  $\Rightarrow$  (2): Trivial.

(2)  $\Rightarrow$  (1): Suppose  $P$  is not finitary, and so there is a  $p \in P$  whose principal ideal  $I$  is infinite. Consider the tree  $T$  of saturated descending chains from  $p$  in  $P$ . For any  $q \in I$ , there is a finite saturated descending chain from  $p$  to  $q$ , because  $P$  is locally finite. Thus, for any  $q \in I$ , there is a distinct path in  $T$ , and since  $I$  is infinite,  $T$  is infinite. Applying the tree version of König’s infinity lemma to this tree, either  $T$  has a vertex of infinite degree or an infinite path. Since  $P$  has finite covers,  $T$  has no vertex of infinite degree. Thus,  $T$  has an infinite path, which is an infinite descending chain from  $p$ .  $\square$

**2.2. The poset of points.** For every instantiation of the general theory of tableau insertion algorithms, we start with a poset  $B$  that is finitary and has finite covers. The elements of  $B$  are called *points*, *boxes*, or sometimes *squares*; the latter terms because at a later stage boxes will be mapped to values, which will be represented graphically by placing values in the boxes. (We reserve the term “cell” for another definition later.)

<sup>1</sup>[GarMcLar1987] provides most of the parts of [McLar1986] dealing with unshifted tableaux, and is more easily available.

<sup>2</sup>[McLar1986] also anticipates parts of [Fom1995].

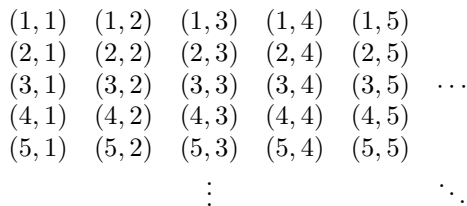
FIGURE 1. The points of the quadrant  $\mathbb{Q} = \mathbb{P}^2$ FIGURE 2. The points of the quadrant  $\mathbb{Q}$  without coordinates

FIGURE 3. Young diagrams

For the “archetype” instantiation of the theory, which is the theory of the Robinson-Schensted algorithm for unshifted tableaux [Schen1961],  $B$  is the quadrant of the plane,  $\mathbb{Q} = \mathbb{P}^2$ , with the order relation

$$(1) \quad (i, j) \leq (k, l) \iff i \leq k \text{ and } j \leq l \quad \text{for all } (i, j), (k, l) \in \mathbb{Q}$$

We display the quadrant in “English format”, as if the elements were the indexes of the elements of a matrix, and sometimes with the boundaries shown explicitly. The locations of the points are displayed as in figure 1. Usually, we display the points without giving their coordinates, as in figure 2.

**2.3. The distributive lattice of diagrams.** A finite order ideal (lower set) of  $B$  is called a *diagram* or *shape*.

In the archetype instantiation, they are also called *Young diagrams* or *Ferrers diagrams*. Examples are shown in figure 3.

The set of all finite order ideals of  $B$ , denoted  $J_f(B)$  [Stan2012, sec. 3.4][Fom1994, Def. 2.1.1], is a distributive lattice, and is the set of all diagrams.  $J_f(B)$  is finitary and because it is a lattice, it has a minimum element, the empty order ideal of  $B$  (which we denote by  $\hat{0}$  or  $\emptyset$ ). Because  $B$  has finite covers,  $J_f(B)$  has finite covers. We set  $V = J_f(B)$  since that will be the set of vertices of graphs that we will define later.  $V$  is naturally graded by  $\rho(x) = |x|$ .

In the archetype instantiation,  $V$  is the lattice of partitions of integers, called *Young’s lattice*  $\mathbb{Y}$ , shown in figure 4.

**2.4. The weight function.** We assume a *weight* function  $w$  from  $B$  to  $\mathbb{P}$  and a *differential degree*  $r \in \mathbb{P}$ .<sup>3</sup>

<sup>3</sup>The operations applied to values of  $w$  (and  $r$ ) are very limited and likely the target of  $w$  could be extended from  $\mathbb{P}$  to any algebraic structure containing a homomorphic image of  $\mathbb{P}$ , with  $r$  also being in the larger structure. In our combinatorial interpretation of  $w$ , this would cause additional complexities, but in the algebraic approach of e.g. [Stan1988], it should be straightforward. See e.g. the signed weights of [Lam2008] and Haiman’s complex-valued weights described in [Stan1990, Prop. 3.3].

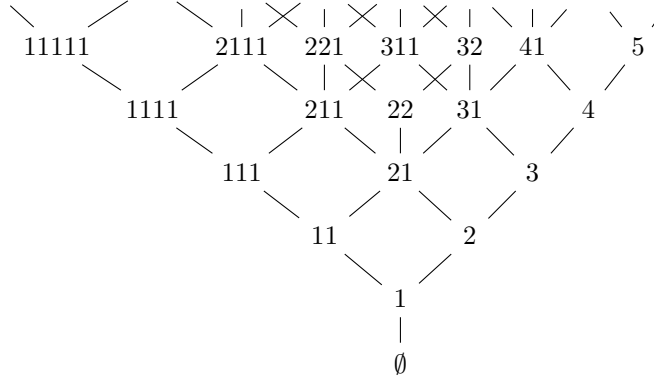


FIGURE 4. Young's lattice  $\mathbb{Y}$  of partitions

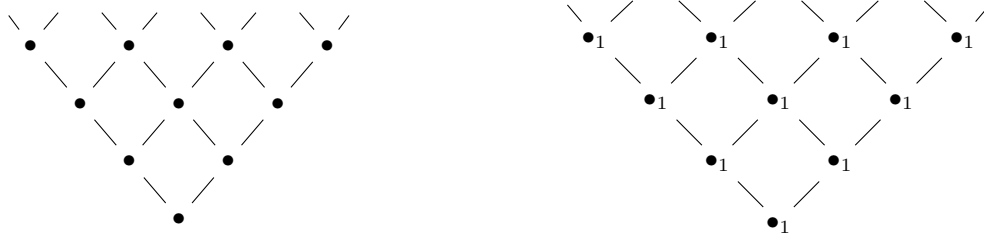


FIGURE 5. (a) Hasse diagram of the quadrant  $\mathbb{Q}$ , (b) with weights  $w(p) = 1$

In order for our constructions to support the conventional counting arguments of paths in the ascending and descending graphs, the weight function must support the algebraic machinery of  $U$  and  $D$  operators in [Stan1988, Def. 1.1] and [Fom1994, sec. 2.2]. This requires

$$(2) \quad \sum_{\substack{y \in V \\ y < x}} w(x - y) + r = \sum_{\substack{z \in V \\ x < z}} w(z - x), \quad \text{for all } x \in V$$

This is a condition relating the weights of the elements of  $B$  that are the differences between  $x$  and the elements of  $V$  it covers to the weights of the elements of  $B$  that are the differences between  $x$  and the elements of  $V$  that cover it. That can be restated as a relationship between the weights of the elements of  $B$  that can be added to  $x$  to make a larger order ideal and the weights of the elements of  $B$  that can be removed from  $x$  to make a smaller order ideal. Because this condition relates several values of  $w$  for each order ideal of  $B$ , it is very restrictive and the space of allowed weight functions for a given  $B$  is usually small.

In the archetype instantiation,  $w(p) = 1$  for all  $p$  and  $r = 1$ , which are the trivial values for  $w$  and  $r$ . The Hasse diagram of the quadrant and the Hasse diagram with the points labeled with their weights are shown in figure 5.

**2.5. The ascending and descending graphs.** We define a directed graph  $G_1$  on the vertex set  $V$  by defining edges for all ascending covering relationships:

$$(3) \quad x \xrightarrow{G_1} y \iff x < y \quad \text{for all } x, y \in V$$

We define a second directed graph  $G_2$  on the vertex set  $V$  by defining edges for all descending covering relationships:

$$(4) \quad x \xleftarrow{G_2} y \iff x < y \quad \text{for all } x, y \in V$$

We conceptualize  $m = w(y - x)$  as the *multiplicity* of edge  $x \xleftarrow{G_2} y$ , labeling each of the multiple edges with a “color” taken from a set of  $m$  elements, often  $[m]$ . The color of an edge  $e$  is denoted  $color(e)$ .

Note that (at this stage of the exposition) edges of  $G_1$  are not multiple and do not have colors.

We abuse the notation by using  $G_1$  and  $G_2$  to denote both the graphs as structures and their sets of edges.

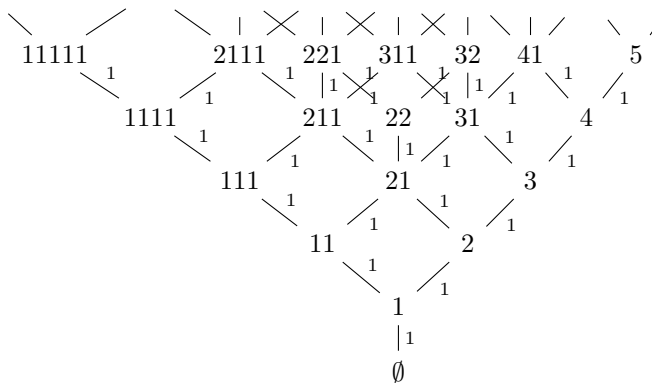


FIGURE 6. The Young graph  $\mathbb{Y}$  with edges labeled with their weights/multiplicities



FIGURE 7. Young tableaux

The structure  $\mathcal{G} = (V, \rho, G_1, G_2)$  forms a *weighted dual graded graph* in the terminology of [Fom1994], which we sometimes abbreviate to *w.d.g.g.* If  $r = 1$ , the w.d.g.g. is a differential poset [Stan1988]. The particular structure and direction of the edges in  $G_1$  and  $G_2$  allow detailed enumeration of directed paths in the graph  $G_1 \uplus G_2$  (on the vertex set  $V$ ) under various constraints. These constraints can be crafted so that the enumerations provide proof of various enumerative identities, often via suitable bijections. See e.g. [Fom1994, sec. 1.5 and 2.9].

In the archetype instantiation,  $G_1$  and  $G_2$  are the graph of covering relations in the lattice of partitions  $\mathbb{Y}$ , with  $G_1$  having the edges directed toward the larger partition and  $G_2$  having the edges directed toward the smaller partition. The edges of  $G_2$  have multiplicity 1 and so are just the reverses of the edges of  $G_1$ . The two graphs can be drawn as in figure 6, with each edge being labeled with its multiplicity in  $G_2$ .

**2.6. Tableaux.** A mapping of the boxes of a diagram to another set, especially  $\mathbb{P}$ , is called a *tableau* (with plural *tableaux*). If the mapping is a bijection into a set  $[n]$ , the tableau is called *standard*.

If a tableau’s mapping is into  $\mathbb{P} \times \mathbb{P}$  and the second component of the value of any point  $p$  in the diagram is  $\in [w(p)]$ , the tableau is called *colored*, with the first component considered the “element” at  $p$  and the second component considered the “color” of the element. If the first component of the values form a bijection into a set  $[n]$ , the tableau is called a *standard colored* tableau.

In the archetype instantiation, tableaux are also called *Young tableaux*, examples of which are shown in figure 7.

**2.7. Growth diagrams.** The next structure we define is a *growth diagram* or *2-growth* [Fom1995, sec. 3.1]. A skeleton growth diagram is shown in figure 8.

Growth diagrams are displayed using the subscripts as Cartesian coordinates, so they are shown in “French format”. Note that the  $g_{i,j}^1$  and  $g_{i,j}^2$  have subscripts that match the higher-numbered node that they connect (to the east or north, resp.), and the  $\alpha_{i,j}$  have subscripts that match the highest-numbered node of the four surrounding them, the one to the northeast. Each group of four nodes together with the four edges between them and the central  $\alpha_{i,j}$  is called a “cell”. A cell extracted from its growth diagram is shown in figure 9.

For a growth diagram of size  $n \times m$ :

- (1) The diagram has a set of *nodes*,  $\{(i, j) : i, j \in \mathbb{N}, 0 \leq i \leq n, 0 \leq j \leq m\}$ .
- (2) Each node is mapped to  $n_{i,j}$ , an element of  $V$ . In a display, the value  $n_{i,j}$  will usually be written at the position of the node.

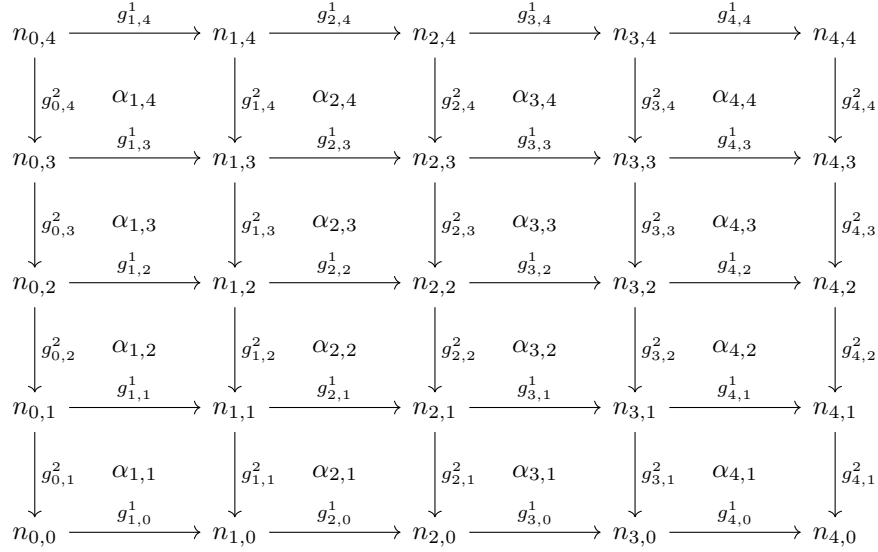


FIGURE 8. A skeleton growth diagram

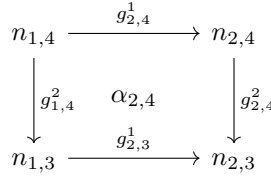


FIGURE 9. A cell extracted from the growth diagram in figure 8

- (3) Each node with  $i = 0$  or  $j = 0$  is mapped to  $\hat{0} \in V$ .
- (4) Each horizontal pair of nodes  $(i - 1, j)$  and  $(i, j)$  is connected by an edge  $g_{i,j}^1$ . If  $n_{i-1,j} = n_{i,j}$ , then  $g_{i,j}^1$  is *degenerate*, contains no further information, and is displayed as an unlabeled arrow. Otherwise,  $g_{i,j}^1$  is mapped to an edge in  $G_1$  from the value  $n_{i-1,j}$  to the value  $n_{i,j}$ . Since the edge is implied by the values  $n_{i-1,j}$  and  $n_{i,j}$ , it is usually displayed as an unlabeled arrow.
- (5) Each vertical pair of nodes  $(i, j - 1)$  and  $(i, j)$  is connected by an edge  $g_{i,j}^2$ . If  $n_{i,j-1} = n_{i,j}$ , then  $g_{i,j}^2$  is *degenerate*, contains no further information, and is usually displayed as an unlabeled arrow. Otherwise,  $g_{i,j}^2$  is mapped to an edge in  $G_1$  from the value  $n_{i,j}$  to the value  $n_{i,j-1}$ . Since the edge is constrained to be one of a set of multiple edges from  $n_{i,j}$  to  $n_{i,j-1}$ , it is usually displayed as an arrow labeled by the color of the edge. When there is only one color for an edge between that pair of elements of  $V$ , the color will often be omitted.
- (6) Each cell is mapped to a value  $\alpha_{i,j}$  in the set  $\mathcal{A} = \{0, 1, \dots, r\} = \{0\} \uplus [r]$ . (This  $r$  is the differential degree, the  $r$  in the constraint equation 2 above.) Usually, the value 0 is considered “null”, whereas the values in  $\mathcal{A}$  that are  $> 0$  are considered “colors”. (Note this is a different definition of “color” than is applied to the edges of  $G_2$ .) When  $\alpha_{i,j} = 0$ , the center of the cell is usually left blank. In the common case  $r = 1$ , the (sole) color 1 is shown as “X”.

Note that the arrows for non-degenerate  $g_{i,j}^1$  and  $g_{i,j}^2$  are shown pointing between the node values in the direction that the edge and nodes are related in  $G_1$  or  $G_2$  (resp.).

In the archetype instantiation, the  $G_2$  arrows are unlabeled, and  $r = 1$ , so all nonzero  $\alpha_{i,j}$  are shown as “X”.

**2.8. Generalized permutations.** A *generalized permutation* [Roby1991, Def. 2.3.6] or *diagonal set* [Fom1994, Def. 2.6.1] is an assignment of values to the  $\alpha_{i,j}$  of a growth diagram such that no two non-zero elements have the

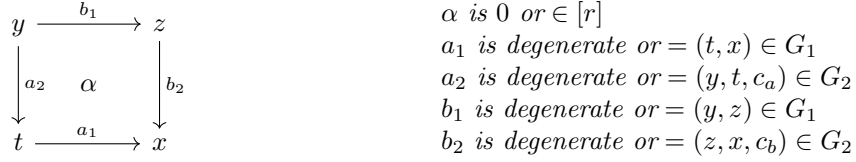


FIGURE 10. Conventional labels of the components of a cell

same first subscript or the same second subscript. (Remember the values  $\alpha_{i,j}$  are  $\in \mathcal{A} = \{0\} \uplus [r]$ .) In all growth diagrams we consider, the  $\alpha_{i,j}$  form a generalized permutation.

A generalized permutation can be represented compactly by listing for each  $j \geq 1$  the value  $i$  (if any) for which  $\alpha_{i,j} \neq 0$  and (if  $r > 1$ ) the value of that  $\alpha_{i,j}$ . For example, the generalized permutation that assigns 1 to  $\alpha_{1,1}$ ,  $\alpha_{2,3}$ , and  $\alpha_{3,2}$ ; assigns 2 to  $\alpha_{4,5}$ ; and 0 to all other  $\alpha_{i,j}$  can be represented  $(1^1, 3^1, 2^1, \dots, 4^2)$ . In terms of an insertion algorithm, this is the insertion of 1, 3, and then 2 during steps 1, 2, and 3, inserting nothing during step 4, then inserting 4 during step 5. In addition, the first three insertions have color 1 and the last insertion has color 2.

In the archetype instantiation, if the dimensions of the growth diagram are equal ( $n = m$ ), a generalized permutation containing  $n$  non-zero  $\alpha_{i,j}$  is an  $n \times n$  permutation matrix. The compact representation of the generalized permutation can omit the colors because they are all 1, resulting in the typical one-line representation of a permutation of  $[n]$ .

**2.9. R-correspondence.** Different authors use similar but not identical terminology for the growth process. We take our terminology from [Roby1991] but with some differences. In this discussion, we mostly consider relations between components of a single cell, and in this context, the conventional labels of the components of a single cell are shown in figure 10 [Fom1995, Lem. 3.7.12 and 4.2.1].

We assume an *R-correspondence*  $\psi$  that is an enumerative expression of the constraint equation 2: For any  $x \in V$ ,  $\psi_x$  is a bijection from

$$\{(x, t, c) \in G_2 : t \leq x \text{ and } c \in [w(x - t)]\} \uplus [r]$$

to

$$\{(z, x, c) \in G_2 : z \succ x \text{ and } c \in [w(z - x)]\}.$$

That is,  $\psi_x$  maps the (multiple) edges in  $G_2$  from  $x$  downward to some  $t$  to a subset of the (multiple) edges in  $G_2$  downward from some  $z$  to  $x$ , and maps the colors used in generalized permutations ( $[r]$ ) to the remaining edges in  $G_2$  downward to  $x$ .

Given the R-correspondence  $\psi$ , we define a function  $\Psi$  that, given the west and south edge values of a cell  $a_1$  and  $a_2$  and the  $\alpha$  value of the cell, determines the cell's north and east edge values  $b_1$  and  $b_2$  of the cell. [Roby1991, sec. 2.6] [Fom1995, sec. 3.4.4 and Lem. 4.2.1] The function  $\Psi$  clearly can be equivalently defined as a mapping from the cell's southwest, northwest, and southeast node values  $x$ ,  $y$ , and  $t$  and west color value  $c_a$  to the northeast node value  $z$  and east color value  $c_b$ :

$$(5) \quad (z, c_b) = \Psi(t, x, y, c_a, \alpha) = \begin{cases} (t, \text{null}) & \text{if } x = y = t \text{ and } \alpha = 0 \\ \psi_x(\alpha) & \text{if } x = y = t \text{ and } \alpha \neq 0 \\ (x, c_a) & \text{if } x \neq t \text{ and } y = t \\ (y, \text{null}) & \text{if } y \neq t \text{ and } x = t \\ \psi_x(x, t, c_a) & \text{if } x = y \neq t \\ (x \vee y, c_a) & \text{if } x \neq y, x \neq t, \text{ and } y \neq t \end{cases} \quad \begin{array}{l} \text{(case "X")} \\ \\ \\ \text{(case "*")} \\ \text{(case "\vee")} \end{array}$$

Given the constraints which we wish growth diagrams to obey, all of the variation allowed in  $\Psi$  is contained within  $\psi$ .

In the archetype instantiation, there is only one color (viz. 1), and we define  $\psi$  as

$$(6) \quad \begin{cases} \psi_x(1) & = x \text{ with a box added to the } 1^{\text{st}} \text{ row} \\ \psi_x(x, t, 1) & = (x \text{ with a box added to the } k + 1^{\text{st}} \text{ row}, x, 1) \\ & \text{when } x \text{ is } t \text{ with a box added to the } k^{\text{th}} \text{ row} \end{cases}$$



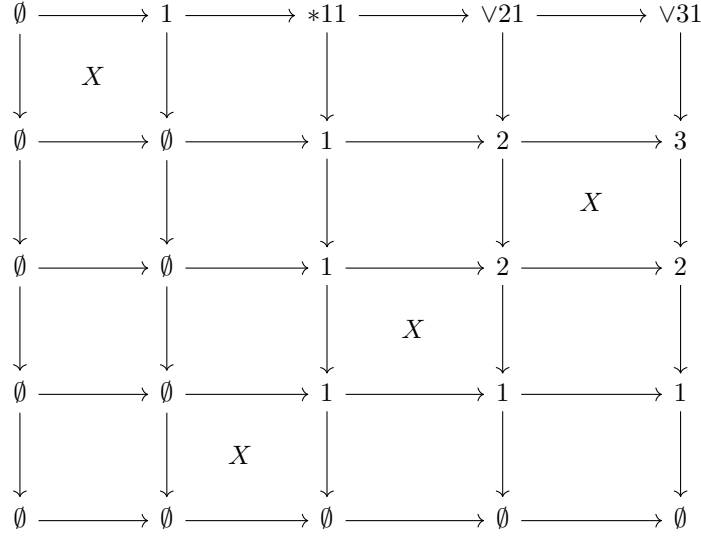


FIGURE 11. Example growth process for the permutation (2, 3, 4, 1). Each  $n$  value is a Young diagram, which is a partition. Each partition is represented by listing its parts, with the empty partition represented by  $\emptyset$ . The cells where  $z = \psi_x(\alpha)$  are marked by “X”. The nodes  $z$  where  $z = \psi_x(x, t, c_a)$  are marked by “\*”. The nodes  $z$  where  $z = x \vee y$  are marked by “∨”. These markings correspond with the marked cases of equation 5.

**2.10. The growth process.** Our primary object of study is the *growth process*, which operates on growth diagrams: Given the function  $\Psi$ , the initial node values  $\hat{0}$  on the west and south sides, and the  $\alpha_{i,j}$ , the remaining values  $g_{i,j}^1$ ,  $g_{i,j}^2$ , and  $n_{i,j}$  can be computed in a wave from the southwest to the northeast of the growth diagram.

The values  $g_{1,m}^1, g_{2,m}^1, \dots, g_{n,m}^1$  (the north edge of the diagram) form a chain of edges in  $G_1$  from  $\hat{0}$  to the vertex  $n_{n,m}$ , which is a diagram. We can form a standard tableau which encodes this chain by mapping each point  $n_{i,m} - n_{i-1,m}$  in  $n_{n,m}$  (the point added by  $g_{i,m}^1$ ) to the value  $i$ . This standard tableau is called the *P tableau*.

The values  $g_{n,m}^2, g_{n,m-1}^2, \dots, g_{n,1}^2$  (the east edge of the diagram) form a chain of edges in  $G_2$  from  $n_{n,m}$  to  $\hat{0}$ . We can form a standard colored tableau which encodes this chain by mapping each point  $n_{n,j} - n_{n,j-1}$  to the value  $(j, color(g_{n,j}^2))$ . This standard colored tableau is called the *Q tableau*.

Intuitively, the northward direction on the growth diagram can be seen as time moving forward, successive insertions done by the insertion algorithm. (Hence the term “growth”.) The value inserted at time step  $j$  (if any) is the  $i$  for which  $\alpha_{i,j} \neq 0$ , and its color is that non-zero value. The shape of the tableaux after the insertion at time  $j$  is  $n_{n,j}$  at the east end of the row.

Intuitively, the westward direction on the growth diagram is “restriction of magnitude”: For all tableau insertion algorithms, the movements and positioning of a value  $i$  in  $P$  is not affected by the insertion of any value  $j > i$ , either before or after the insertion of the  $i$ . Truncating the growth diagram at column  $i_{max}$  shows the shape of  $P$  as if none of the values  $> i_{max}$  were inserted, or equivalently, if all boxes with values  $> i_{max}$  in  $P$  are deleted.

In the archetype instantiation, the generalized permutation (2, 3, 4, 1) that assigns 1 to  $\alpha_{2,1}$ ,  $\alpha_{3,2}$ ,  $\alpha_{4,3}$ , and  $\alpha_{1,4}$ ,<sup>4</sup> and 0 to all other  $\alpha_{i,j}$  generates the growth process shown in figure 11. This growth generates the *P* and *Q* tableaux shown in figure 12.

**2.11. Relationship of R-correspondences to insertion algorithms.** The three marked cases of equation 5 implement the features of an insertion algorithm [Fom1995, sec. 4.2 and 4.4]:

case “X” – This case shows where in the diagram a value will be inserted, if the value is larger than all values already in the tableau. (Remember that generalized permutations contain no duplicated values.)  $t = x = y$

<sup>4</sup>Remember that in a growth diagram, the coordinates are assigned in the Cartesian manner.

1	3	4
2		

1	2	3
4		

FIGURE 12.  $P$  and  $Q$  tableaux generated by the example growth process of figure 11

is the tableau before insertion, and  $z$  is the tableau after the insertion. Additionally, the  $b_2$  edge shows *how* the value is inserted, for algorithms in which insertions can be done in more than one way. This information is propagated to cells to the east, that is, to further steps in the overall insertion of that one element, and ultimately becomes the color of the corresponding element of the  $Q$  tableau. Thus, the  $b_2$  edge and edges eastward carry the state information during the insertion of one number.

case “\*” – This case shows what happens when a value is inserted but that insertion conflicts with the previous insertion of a larger value. In general, the new, smaller value will be inserted in the same place it would have been inserted if the larger value was not present, and the larger value is displaced, *bumped*, into another place. The  $a_2$  edge shows where the smaller value is inserted, and the  $b_2$  edge shows the new location of the previous, larger value.

case “ $\vee$ ” – This case is when a value is inserted and a larger value has been inserted previously, but the two insertions do not conflict.

In the archetype instantiation, consider the example growth given in figure 11. The generalized permutation is  $(2, 3, 4, 1)$ . Because  $r = 1$  there are only one color in the generalized permutation, and the  $G_2$  edges have only one color, which is not shown; i.e. all insertions are “done in the same way”.

The southern row corresponds to the first insertion of the Robinson-Schensted insertion, when 2 is inserted into an empty tableau. The westernmost cell has all nodes  $\emptyset$ , because when only elements  $\leq 1$  are considered, no change happens. The next cell east shows 1 being inserted into  $\emptyset$  to form the tableau 1. The remaining cells to the east show that successively allowing consideration of larger elements causes no change, as at this time, no larger elements have been inserted. The tableau after the insertion has the shape given as northeast node of the last cell, 1. The  $P$  tableau at this stage in time, which is 1, is constructed by the nodes at the northern side of the row. The  $Q$  tableau, which is 1, is constructed by the nodes from the southeast corner to the northeast node of the last cell in the row.

A more complicated case is the northern row, where 1 is inserted into the tableau 

2	3	4
---	---	---

 of shape 3. The westernmost cell in the row shows the insertion of 1, with elements  $> 1$  being ignored, giving the shape 1. The next cell shows how the insertion of 1 interacts with the previous insertion of 2; the 2 is bumped into the second row. That this is a bump is shown by the nodes of the cell having  $x = y > t$ . The R-correspondence sets  $z$  to 11, meaning that the bumped element is moved to the next row. The third cell shows the interaction of the insertion of 1 with the insertion of 3. In this case, the 3 is unaffected. This is shown by the nodes of the cell having  $x \neq y$ . The  $z$  is constructed by  $x \vee y$ . The fourth and easternmost node of the row is similar to the third.

A more complex example is the first instantiation for shifted tableaux 6.1, in which the  $G_2$  edges have non-trivial labels, shown as “ $B$ ”, “ $R$ ”, and “ $-$ ” in figure 32. Since the  $G_2$  edges are north-south edges between nodes, during a growth, the information in an edge propagates eastward, that is it is state information during the insertion process, generated during the initial insertion of an element into the tableau, possibly modified by bumping operations, and finally recorded in the  $Q$  tableau. But that state is not affected by the state of earlier (more southern) insertions and does not affect the state of later (more northern) insertions.

### 3. DUALITY

**3.1. Inversion duality.** Since the values  $\alpha_{i,j}$  form a permutation matrix, it is well known that the inverse of that permutation is  $\alpha_{i,j}^{-1} = \alpha_{j,i}$ . Geometrically, this is transposing the matrix of  $\alpha$  values around the southwest-northeast axis. Thus, since  $(4, 1, 2, 3)$  is the inverse of  $(2, 3, 4, 1)$ , the  $\alpha$  values in the growth process shown in figure 13 are the transpose of the  $\alpha$  values in the growth process shown in figure 11:  $\alpha'_{i,j} = \alpha_{i,j}$ .

If  $w(p) = 1$  for all  $p$ , and it is in the archetype instantiation, there are effectively no labels on the  $G_2$  edges in the growth diagram, and applying  $\Psi$  to construct the growth process to the inverse permutation constructs the same node values as in the growth process for the original permutation, but in the transposed locations:  $n'_{i,j} = n_{j,i}$ .

The result is that the  $P$  and  $Q$  tableaux for the inverse permutation are the  $Q$  and  $P$  (resp.) tableaux for the original permutation.

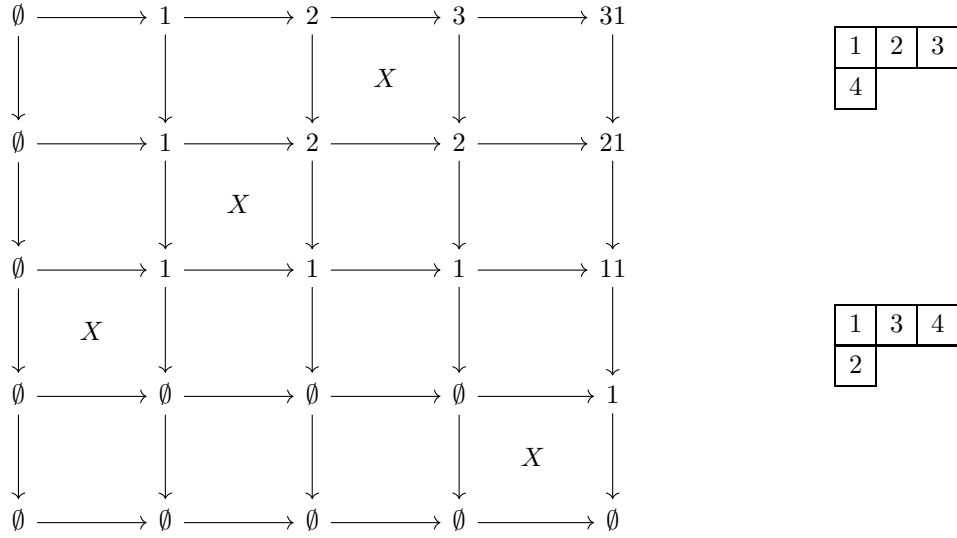


FIGURE 13. Example growth process for the permutation  $(4, 1, 2, 3)$ , which is the inverse of  $(2, 3, 4, 1)$  in figure 11: (a) growth diagram, (b)  $P$  tableau, and (c)  $Q$  tableau

Note that inversion duality does not transpose the shapes that are the  $n_{i,j}$  values, nor the shapes of the  $P$  or  $Q$  tableaux.

**3.2. Transpose duality.** A completely distinct (but confusingly similar) duality for instantiations using unshifted tableaux is “transpose duality”, which is conceptually the application of the transpose automorphism to  $\mathbb{Q}$  and  $V$  and making the parallel changes to  $\Psi$  and  $\psi$ :

$$(7) \quad \begin{cases} \psi_x^T(\alpha) & = (z^T, x, c) & \text{where } (z, x^T, c) = \psi_{x^T}(\alpha) \\ \psi_x^T(x, t, c) & = (z^T, x, c) & \text{where } (z, x^T, c) = \psi_{x^T}(x^T, t^T, c) \end{cases}$$

$$(8) \quad \Psi^T(t, x, y, c_a, \alpha) = \Psi(t^T, x^T, y^T, c_a, \alpha)$$

No insertion algorithm is self-dual under transpose duality. But if the transpose-dual of an algorithm is applied to a permutation, the resulting growth diagram’s node values are the transposes all of the node values of the growth diagram generated by the original algorithm, and the resulting  $P$  and  $Q$  tableaux are the transposes of the  $P$  and  $Q$  tableaux generated by the original algorithm. The canonical example of transpose duality is the relationship between “row insertion” 5.1 and “column insertion” 5.2 for unshifted tableaux.

There is also an extended sense of transpose duality where in addition to transposing the shapes, a bijection is applied to the colors of the elements of the generalized permutation, and a bijection is applied to the  $G_2$  edges and the colors of the elements of  $Q$ :

$$(9) \quad \begin{cases} \psi_x^T(\alpha) & = (z^T, x, g(c)) & \text{where } (z, x^T, c) = \psi_{x^T}(f(\alpha)) \\ \psi_x^T(x, t, c) & = (z^T, x, g(c)) & \text{where } (z, x^T, c) = \psi_{x^T}(x^T, t^T, g^{-1}(c)) \end{cases}$$

#### 4. THE INSERTION DIAGRAM FOR AN INSERTION ALGORITHM

We next show a convenient way of displaying an R-correspondence  $\psi$  that specifies  $\psi_x$  for each shape  $x$ .

Fundamental to defining  $\psi_x$  are the shapes  $x^-$  covered by  $x$  in  $V$ , the shapes  $x^+$  that cover  $x$ , and the set of colors of non-zero elements of generalized permutations  $\alpha$  (which is  $[r]$ ).

In the archetype instantiation for unshifted tableaux, we can choose as an example  $x$  the shape  $(5, 3, 3, 1)$ , shown in figure 14(a). We label the points which can be removed from  $x$  to form the shapes  $x^- < x$  with “-” and label the points that can be added to  $x$  to form the shapes  $x^+ > x$  with “+”, as in figure 14(b). The points  $x^-$  that can be removed from  $x$  are maximal in  $x$ ; we also call them *deletion points* of  $x$ . The points  $x^+$  that can be added to  $x$  are *cominimal*, the minimal points in the complement of  $x$  (with respect to  $B$ ); we also call them *insertion points* of  $x$ .

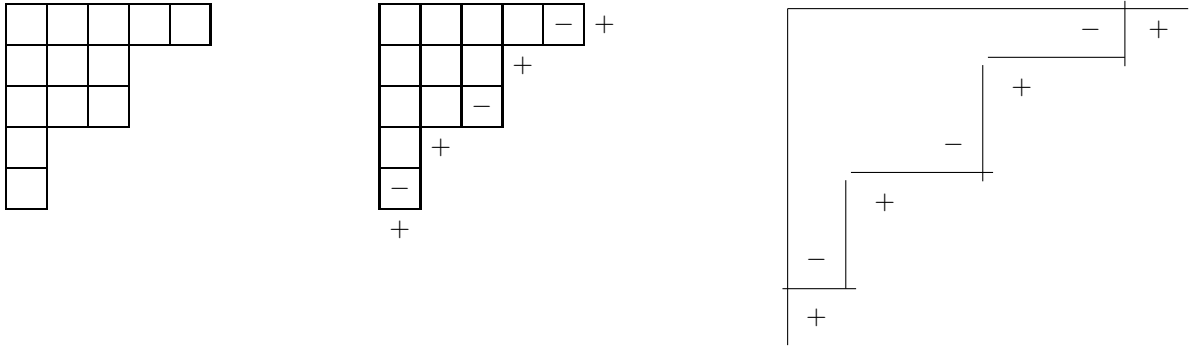


FIGURE 14. (a) The shape  $(5, 3, 3, 1)$ , (b) its maximal and cominimal points, (c) the same shown more abstractly

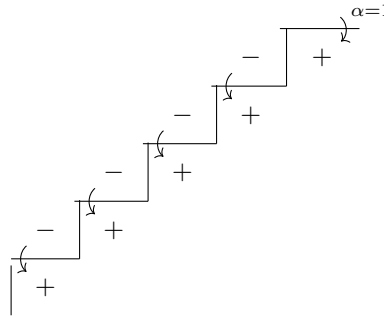


FIGURE 15. Generic insertion diagram for Robinson-Schensted (row) insertion



FIGURE 16. Cells (a) representing insertion and (b) representing bumping

For unshifted tableaux, the diagrams for all shapes  $x$  have a similar pattern of maximal and cominimal points, viz. progressing from northeast to southwest, they alternate, with a “+” at both the northeast and southwest ends. For each “-”, there is a “+” in the next row south of it and a “+” in the next column east of it. This generic pattern is shown in the more abstracted figure 14(c).

For the archetype instantiation, we can create an *insertion diagram* for the Robinson-Schensted insertion algorithm showing the generic  $\psi$  as in figure 15. It encodes  $\psi_x$  via:

case “X” – For the one  $\alpha$  color 1, consider  $\psi_x(1) = (x^+, x, c) \in G_2$  where  $x^+ = x \uplus \{q\}$ . In the insertion diagram, there is an unanchored arrow, labeled with “ $\alpha = 1$ ”, to the point  $q$  in the northeast. If  $w(q) > 1$ , the edge  $x \xleftarrow{G_2} x^+$  is multiple, we would also label this edge with the color  $c$  that selected that edge in  $G_2$ , but for unshifted tableaux,  $w(q) = 1$ . Arrows of this form specify the processing of cells where  $\alpha \neq 0$  as in figure 16(a).

case “\*” – Now consider  $(x, x^-, c) \in G_2$  where  $x^- = x \setminus \{p\}$  and  $c \in [w(p)]$ . The value  $\psi_x(x, x^-, c) = (x^+, x, c') \in G_2$  for some  $x^+ = x \uplus \{q\}$  and  $c' \in [w(q)]$ . In the insertion diagram, there is an arrow from  $p$  (which is a maximal point of  $x$ ) to  $q$  (which is a cominimal point of  $x$ ). We label the arrow with the combination  $c/c'$  to show the colors of the “downward from  $x$ ” and “downward to  $x$ ” edges, respectively. If

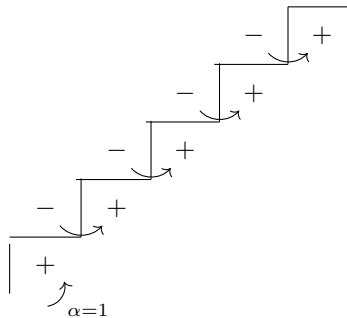


FIGURE 17. Generic insertion diagram for column insertion into unshifted tableaux

either  $w(p) = 1$  or  $w(q) = 1$ , we omit  $c$  or  $c'$  from the label (resp.) and for the archetype instantiation, we can omit the label entirely. Arrows of this form specify the processing of cells where  $\alpha = 0$  as in figure 16(b).

In order for the arrows of an insertion diagram to define an acceptable  $\psi_x$ , the following constraints must be met:

- (1) There must be one “ $\alpha = \cdot$ ” arrow to some insertion point for each  $\alpha$  color.
- (2) For each deletion point  $p$ , there must be  $w(p)$  arrows in the diagram leading from it, with one labeled with each of the colors in  $[w(p)]$ .
- (3) For each insertion point  $q$ , there must be  $w(q)$  arrows in the diagram leading to it, with one labeled with each of the colors in  $[w(q)]$ .

For an instantiation, there need not be a single generic pattern for the insertion diagrams for all  $x \in V$ . As [McLar1986] emphasizes, an insertion diagram could be independently chosen for each  $x$ , and the assemblage of them would define an R-correspondence  $\psi$  for the w.d.g.g.  $\mathcal{G}$ . Since  $V$  is countably infinite, there are a continuum number of possible  $\psi$ . Nonetheless, the more interesting insertion algorithms have very systematic R-correspondences which can be represented by one or a few generic insertion diagrams.

Of course, insertion diagrams provide no more information than specifying  $\psi$  directly (e.g. as in [Fom1995, sec. 4.2 and 4.5]), but they provide the information in a way that is much more intuitively accessible, as will be shown in later sections that discuss various instantiations of the theory.

As [McLar1986] notes, all R-correspondences for a particular lattice of diagrams and weight function prove the same basic enumeration formulas. However, a particular R-correspondence may have distinct enumerative value if it transforms an interesting subset of permutations into an interesting subset  $P/Q$  pairs.

## 5. UNSHIFTED TABLEAUX ALGORITHMS

**5.1. Robinson-Schensted insertion.** The archetype instantiation of an insertion algorithm is Robinson-Schensted insertion for unshifted tableaux [Schen1961], also called “row insertion” and “Schensted insertion” in [Haim1989, sec. 2]. Its generic insertion diagram is shown in shown in figure 15.

**5.2. Column insertion.** Similarly, the generic insertion diagram for the “column insertion” variant of the Robinson-Schensted algorithm for unshifted tableaux is shown in figure 17. Note that in this paper, all sequences of inserted values are generalized permutations and so have no repeated values (and so we do not attach Knuth’s name to the algorithms). Thus, column insertion is the transpose-dual of row insertion, which can be seen by the fact that its insertion diagram, figure 17, is the transpose of the insertion diagram of row insertion, figure 15.

**5.3. Haiman’s left-right insertion.** Given a particular lattice of diagrams  $V$ , the weight equation 2 is linear on the differential degree  $r$  and the weight function  $w$  together. The archetype instantiation has  $r = 1$  and  $w(p) = 1$ , so another instantiation on the lattice of Young diagrams is the “double” of it,  $r = 2$  and  $w(p) = 2$ .

Haiman [Haim1989, sec. 4] constructed an insertion algorithm for this doubled instantiation that is a combination of row and column insertion, called “left-right insertion”. Since  $r = 2$ , there are two colors in the generalized permutation, with  $\alpha = 1$  called uncircled and  $\alpha = 2$  called circled. Uncircled elements are inserted with row insertion and circled elements are inserted with column insertion, with the elements’ circling recorded in the  $Q$  tableau. The insertion diagram for left-right insertion is a straightforward combination of the insertion diagrams for row and

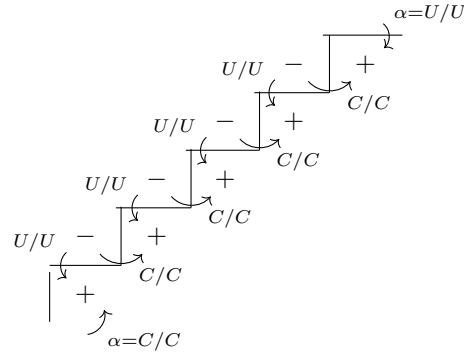


FIGURE 18. Generic insertion diagram for left-right insertion

column insertion, as shown in figure 18, where the edges in  $G_2$  have two labels, represented “ $U$ ” and “ $C$ ”, and the values of  $\alpha$  are similarly represented by “ $U$ ” and “ $C$ ”.

An example of a left-right insertion as a growth diagram is figure 19. Note that for any insertion/bump sequence, the colors of all  $G_2$  edges in that row of the growth are the same, and the circling of an element  $i$  in the  $Q$  tableau is the same as the circling of the  $i$ -th element of the generalized permutation, which created it.

Left-right insertion has transposition duality when the circling of all elements of the generalized permutation is inverted. This can be seen by inspecting the insertion diagram figure 18: transposing it and replacing all “ $U$ ” with “ $C$ ” and vice-versa leaves it unchanged.

**5.4. McLarnan’s fairy insertion.** [McLar1986] and [GarMcLar1987] introduce “generic” insertion algorithms, parameterized algorithms that generate a family of different insertion algorithms. Any such family makes it easy to define many algorithms with baroque and unusual structures. These aspects resemble the creation of unconventional pieces in fairy chess so we call these algorithms “fairy” algorithms.

[McLar1986, Fig. 1.4] and [GarMcLar1987, Fig. 4] illustrate a relatively simple fairy algorithm. The generic insertion diagram for this algorithm is figure 20 and is not as visually simple as for other algorithms; the arrows from the deletion points to the insertion points, instead of preserving the order of the two sets, reverse it, reserving the northeastmost insertion point as the “ $\alpha = \cdot$ ” point. In McLarnan’s words,

A slightly more complex bumping scheme might take the bottom removable square to the top addible square, the second lowest removable square to the second highest addible square, and so on. For this scheme as for the row insertion bumping scheme, the lone square is always in the first row.

An example of the algorithm is figure 21, taken from [GarMcLar1987, Fig. 7].

**5.5. Jitter fairy insertion.** Other algorithms we catalog here leave the labels (circling) unchanged for most bumping operations, occasionally changing labels when a bump involves the northeast or southwest corner of the tableau. We now construct a fairy algorithm that changes labels for *all* bumps, and label it *jitter insertion*. The generic insertion diagram for this algorithm is figure 22. It resembles left-right insertion 5.3, except that every time a number is inserted or bumped, its circling is reversed, and so the next time the number is bumped, it will move in the reverse direction in the tableau. Examples of this algorithm are figures 23, 24, 25, and 26.

## 6. SHIFTED TABLEAUX ALGORITHMS

Further instantiations of the theory use *shifted tableaux*. For these instantiations,  $B$  is the “octant” of the plane,  $\mathbb{O} = \{(i, j) \text{ where } i, j \in \mathbb{P} \text{ and } i > j\}$ , with the same order relation as the quadrant,

$$(10) \quad (i, j) \leq (k, l) \iff i \leq k \text{ and } j \leq l \text{ for all } (i, j), (k, l) \in \mathbb{O}$$

Like the quadrant, we display the octant in “English format”, with the locations of the points displayed as in figure 27. The lattice of diagrams  $V$  is the lattice of shifted Young diagrams,  $\mathbb{S}\mathbb{Y}$ . Example *shifted Young tableaux* are shown in figure 28.

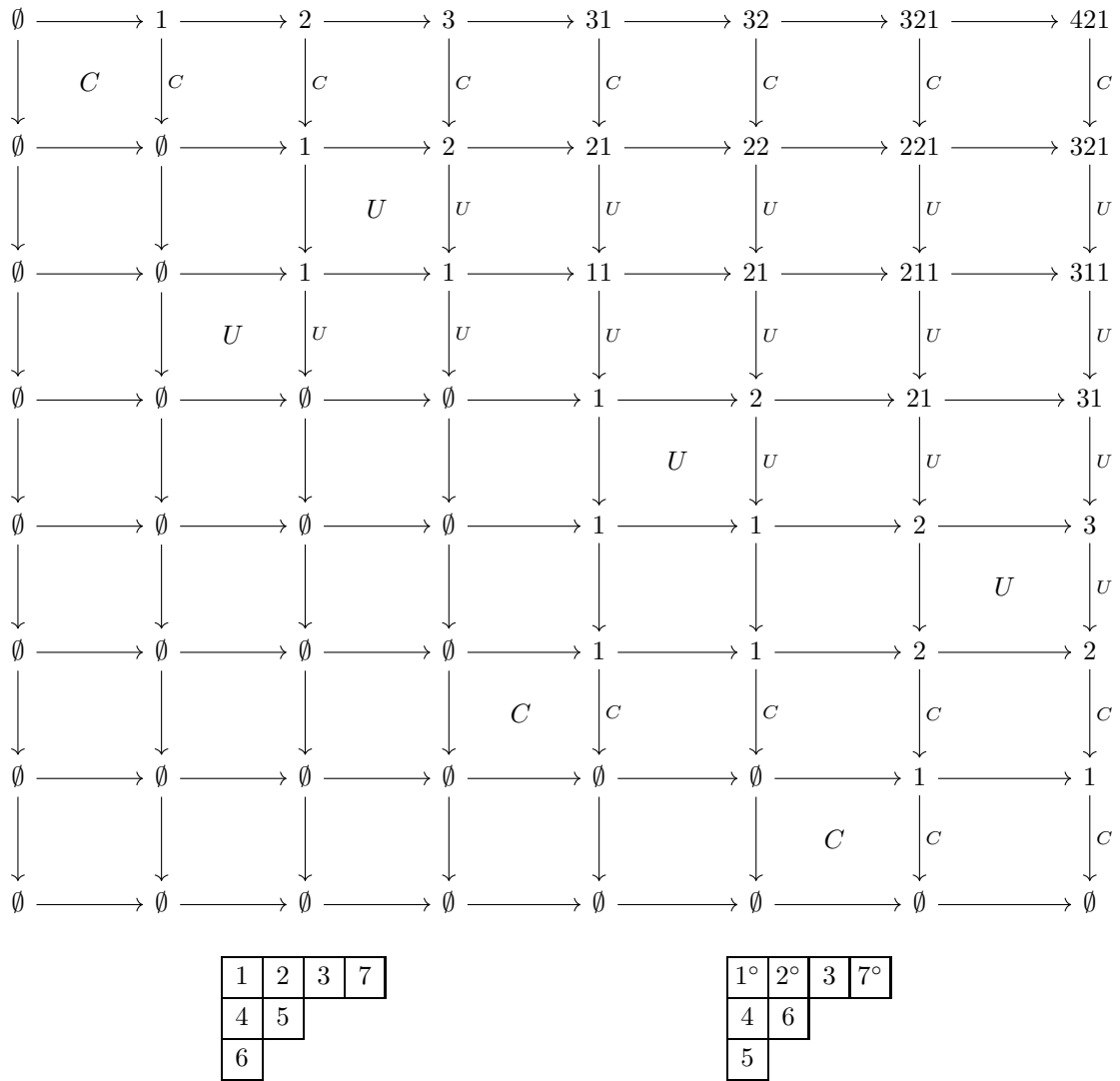


FIGURE 19. Growth for the permutation  $(6^\circ, 4^\circ, 7, 5, 2, 3, 1^\circ)$  for left-right insertion: (a) growth diagram, (b)  $P$  tableau, and (c)  $Q$  tableau

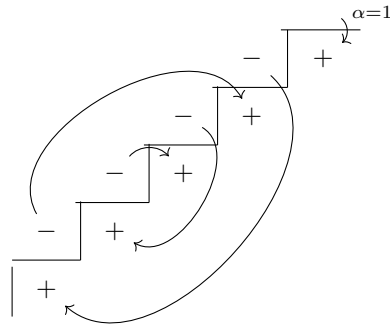


FIGURE 20. Generic insertion diagram for McLarnan's fairy insertion

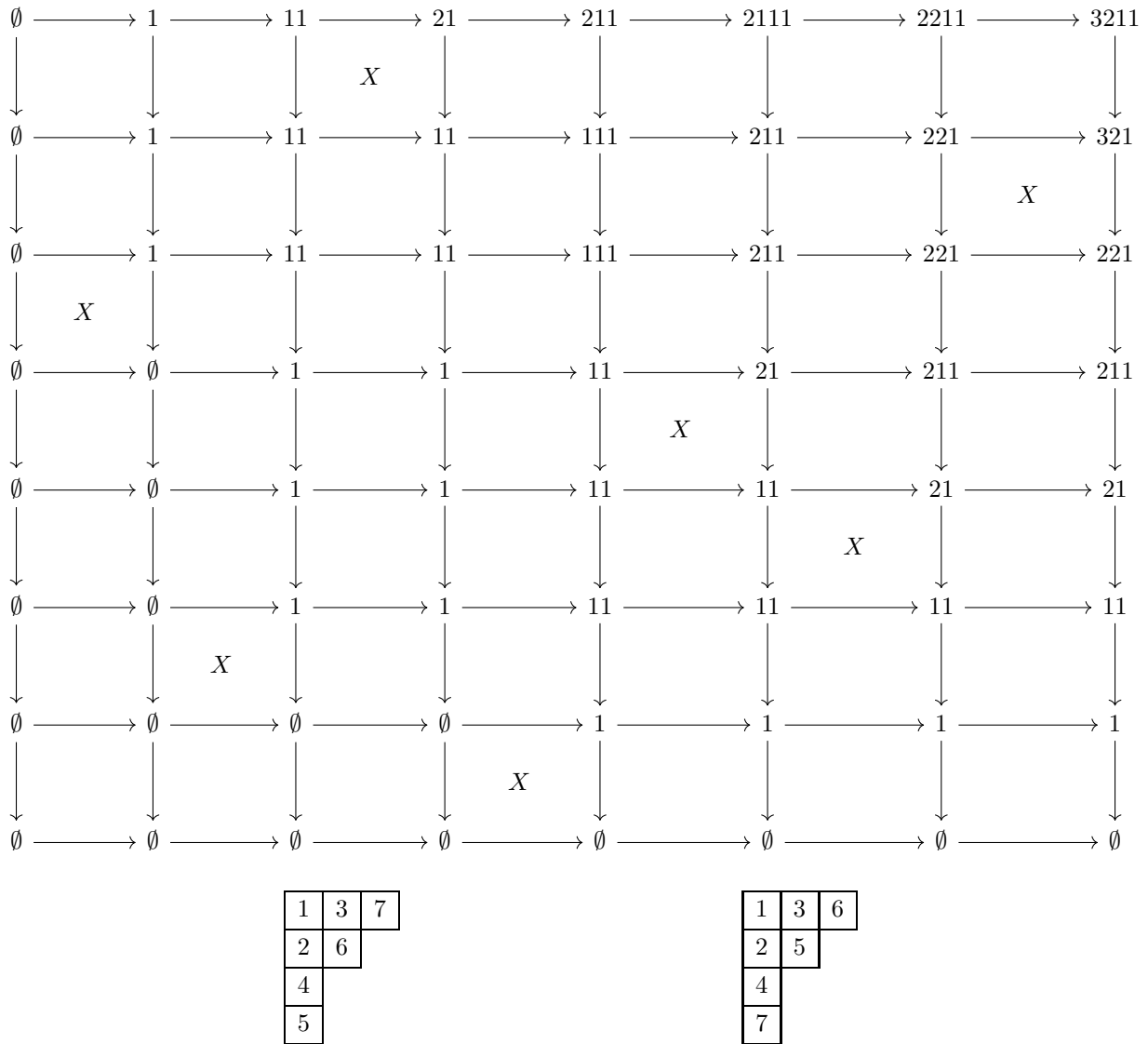


FIGURE 21. Growth for the permutation  $(4, 2, 6, 5, 1, 7, 3)$  for McLarnan's fairy insertion: (a) growth diagram, (b)  $P$  tableau, and (c)  $Q$  tableau

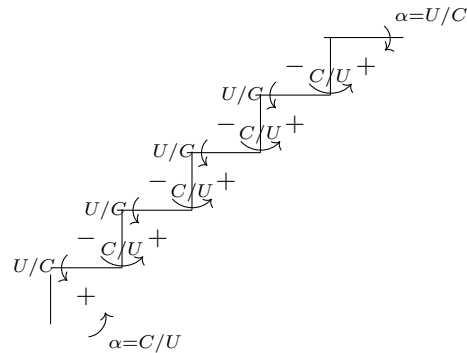


FIGURE 22. Generic insertion diagram for the "jitter" insertion



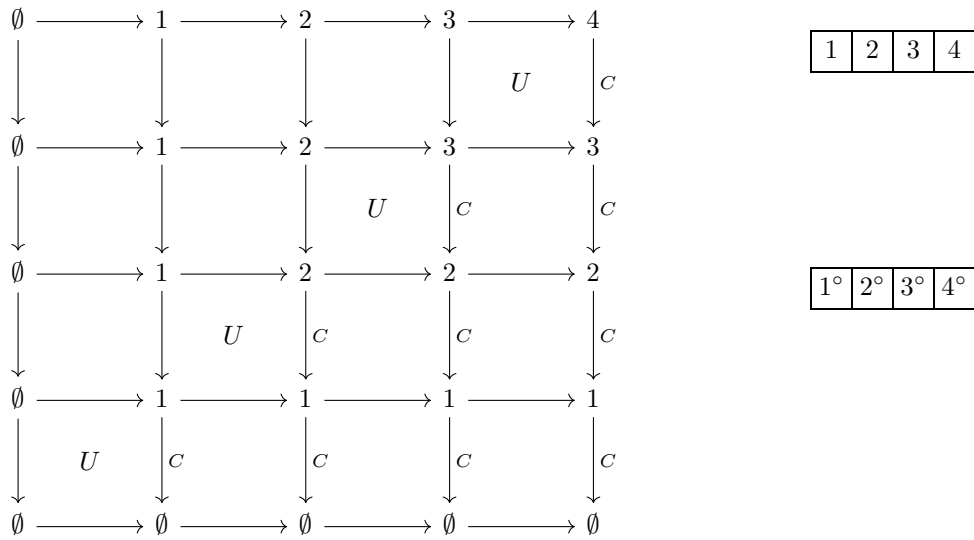


FIGURE 23. Growth for the permutation  $(1, 2, 3, 4)$  for the “jitter” algorithm: (a) growth diagram, (b)  $P$  tableau, and (c)  $Q$  tableau

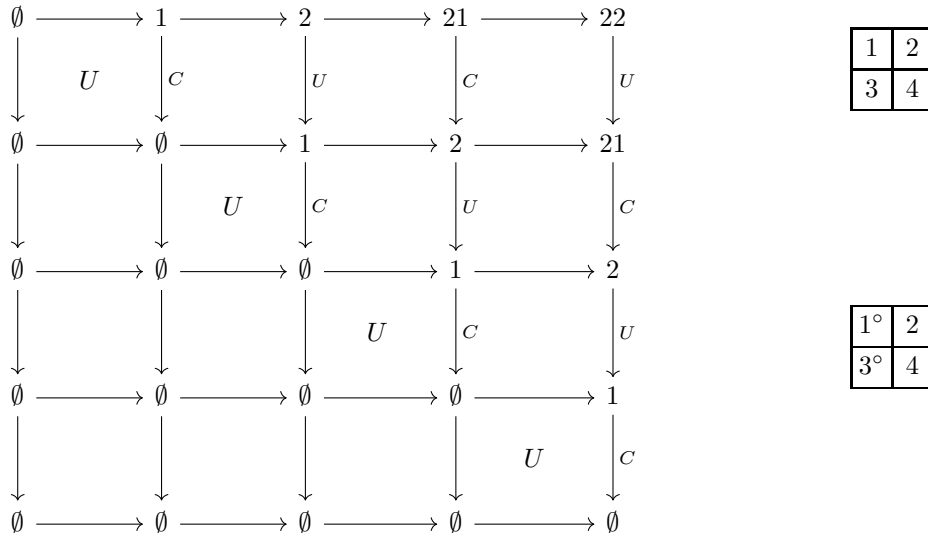


FIGURE 24. Growth for the permutation  $(4, 3, 2, 1)$  for the “jitter” algorithm: (a) growth diagram, (b)  $P$  tableau, and (c)  $Q$  tableau

The only weight function on this  $B$  compatible with differential degree  $r = 1$  is [Stan1990, sec. 3][Fom1994, Exam. 2.2.8]

$$(11) \quad w(p) = \begin{cases} 1 & \text{if } p \text{ is on the diagonal} \\ 2 & \text{otherwise} \end{cases}$$

The Hasse diagram of the octant with the points labeled with their weights is figure 29. The dual graded graph with the edges labeled with their multiplicities in  $G_2$  is shown in figure 30.

For colored shifted Young tableaux, the the main-diagonal points have weight 1 and so their values always have the same color. The off-diagonal points have weight 2 and so their values can have two colors. In [Sag1979] the values of point with color 2 are made members of a set of distinguished values. In other works dealing with shifted tableaux

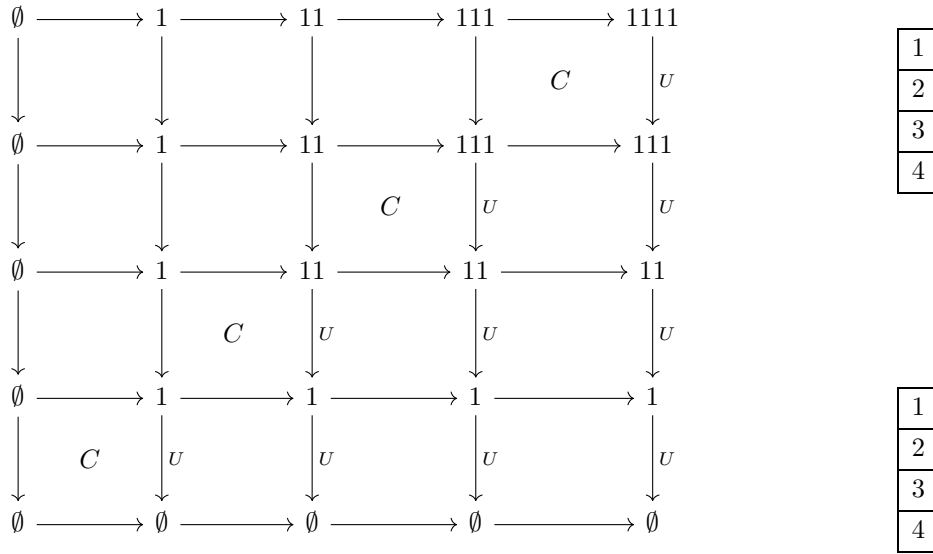


FIGURE 25. Growth for the permutation  $(1^\circ, 2^\circ, 3^\circ, 4^\circ)$  for the “jitter” algorithm: (a) growth diagram, (b)  $P$  tableau, and (c)  $Q$  tableau

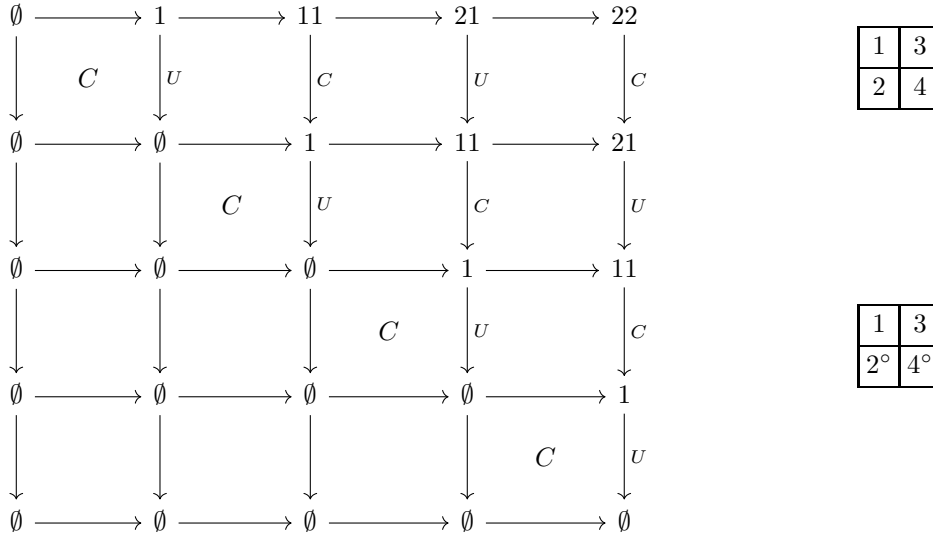


FIGURE 26. Growth for the permutation  $(4^\circ, 3^\circ, 2^\circ, 1^\circ)$  for the “jitter” algorithm: (a) growth diagram, (b)  $P$  tableau, and (c)  $Q$  tableau

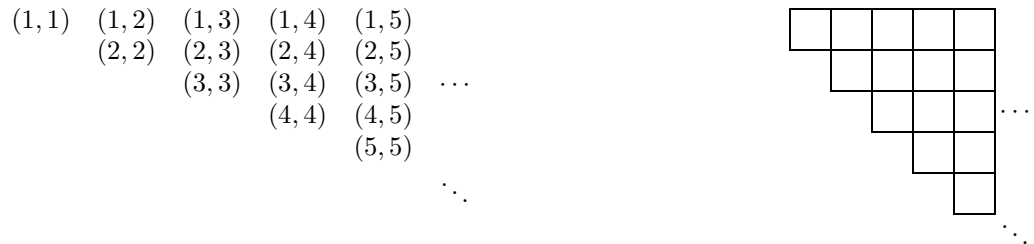


FIGURE 27. The points of the octant  $\mathbb{O}$  with and without coordinates

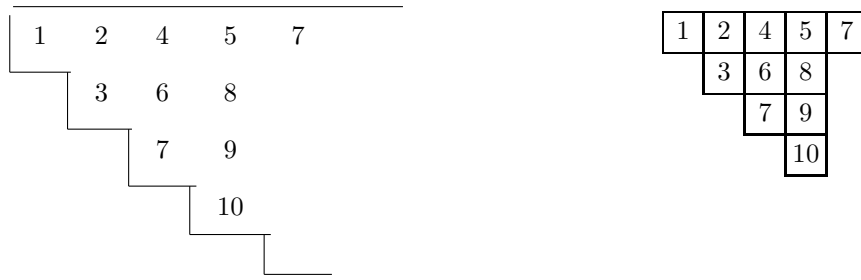


FIGURE 28. Shifted Young tableaux

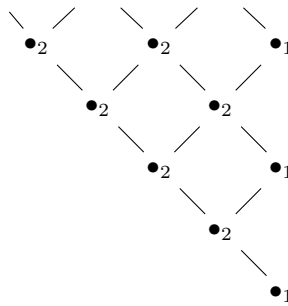


FIGURE 29. The Hasse diagram of the octant  $\mathbb{O}$  with weights  $w(p) = 1$  for diagonal elements and 2 for other elements

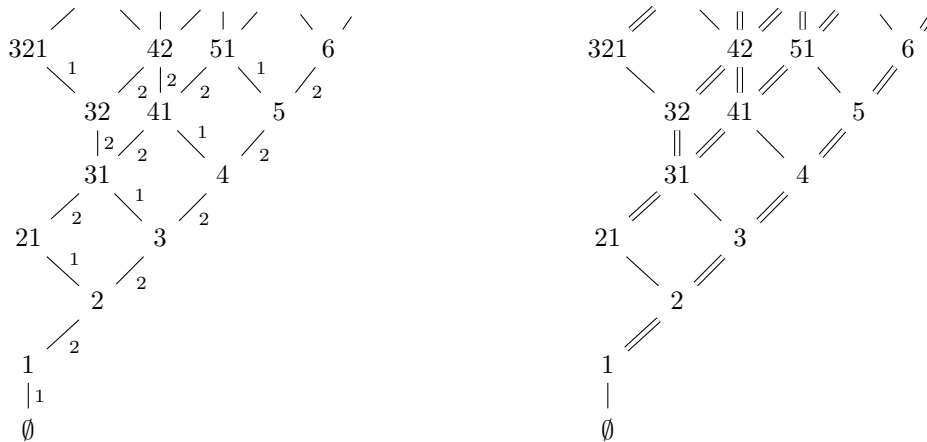


FIGURE 30. The graph of strict partitions  $\mathbb{S}\mathbb{Y}$  (a) with edges labeled with their weights/multiplicities and (b) with edges shown multiply

the values with color 2 are considered marked in some manner, usually as being *circled*. Here we show off-diagonal points with color 2 as “circled” with a superscript “degree” symbol:  $\cdot^{\circ}$  (resembling [Haim1989, sec. 2]).

**6.1. Sagan’s first algorithm for shifted tableaux.** One insertion algorithm for shifted tableaux is Sagan’s first algorithm [Sag1979]. A thumbnail description is:

- (1) A number being inserted into the  $P$  tableau is inserted into the first row, with any (larger) number that it bumps being inserted into the second row, etc. as for row insertion into unshifted tableaux.

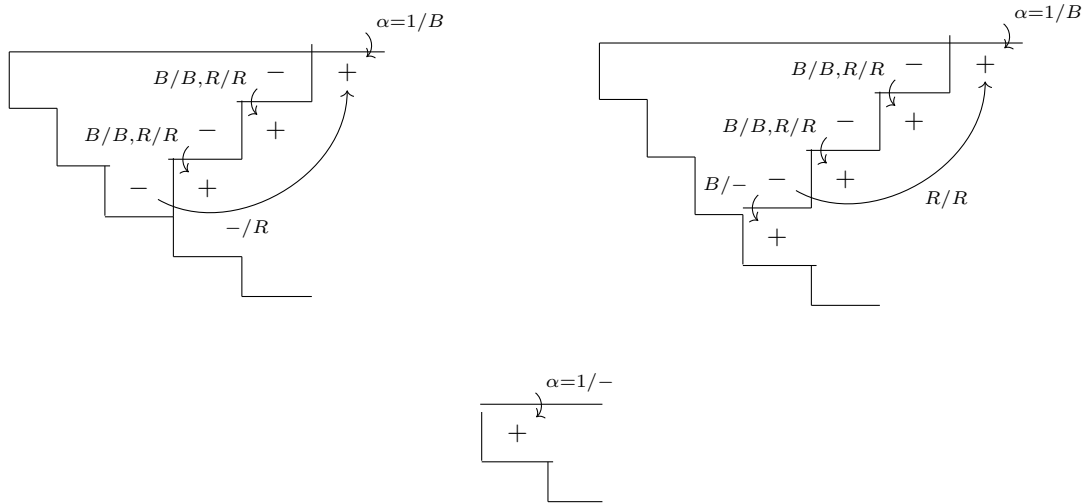


FIGURE 31. Generic insertion diagrams for Sagan's first algorithm: (a) last part of  $x = 1$ , (b) last part of  $x > 1$ , and (c)  $x = \emptyset$ , which is a special case of (b)

- (2) However, if a number is inserted into the main diagonal cell of a row and bumps a number, that larger number begins another sequence of row insertions, starting with the first row, but now with the constraint that if a number would be inserted into a main diagonal cell, it instead is returned to the first row to start a new sequence of row insertions.

This insertion algorithm can be summarized straightforwardly in the insertion diagrams shown in figure 31. They show directly that the insertion algorithm is invertible and that 2 is satisfied for  $r = 1$ . Note these points about the insertion diagram:

- (1) There are two distinct generic insertion diagrams, because the pattern of insertion and deletion points differs depending on whether the shape has a (last) row with length 1 or not. (The shapes that do not are  $\emptyset$  and shapes with a last row with length  $> 1$ .) The third insertion diagram shows how the special case  $\emptyset$  works out.
- (2) The points on the main diagonal have weight 1, and so all edges to such points in  $G_2$  have the same color. Following [Fom1995, sec. 4.5], we call the color of those edges "black", which we abbreviate "-" in the insertion diagrams.
- (3) The points not on the main diagonal have weight 2. Each such point has two edges in  $G_2$ , which again following [Fom1995, sec. 4.5], we call the color of those edges "blue" and "red", which we abbreviate "B" and "R" in the insertion diagrams.
- (4) From some of the deletion points, the blue and red edges lead to the same insertion point, so a single arrow is shown with the two "before/after" color specifications combined.
- (5) It is a straightforward visual exercise to verify that these insertion diagrams satisfy the constraints required to specify a valid  $\psi$ .
- (6) The insertion diagram shows the general pattern of bumps generated by an insertion: The " $\alpha = \cdot$ " edge shows that the element is inserted into the first row as a blue insertion. Successive bumps are blue insertions into successive rows until a main diagonal element is bumped, at which point the bumped element is inserted into the first row as a red insertion. Bumps caused by red insertions remain red insertions, and never are inserted as main diagonal elements.

The growth for the example permutation  $(1, 2, 5, 4, 3)$  and the resulting tableaux are shown in figure 32.

**6.2. The second algorithm for shifted tableaux.** A second insertion algorithm for shifted tableaux was discovered independently<sup>5</sup> by Worley [Wor1984] and Sagan [Sag1987]. A thumbnail description is:

<sup>5</sup>And nearly simultaneously: A letter from Sagan to Richard Stanley reporting his discovery crossed in the mail with a letter from Stanley to Sagan reporting Worley's discovery.

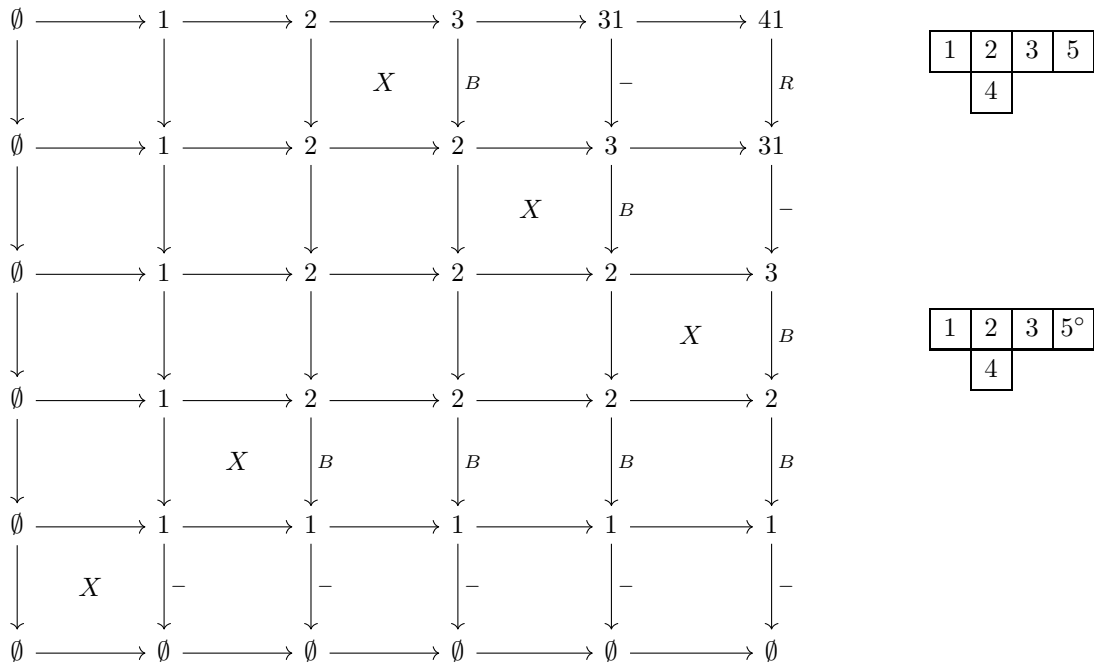


FIGURE 32. Growth for the permutation  $(1, 2, 5, 4, 3)$  for Sagan's first algorithm: (a) growth diagram, (b)  $P$  tableau, and (c)  $Q$  tableau

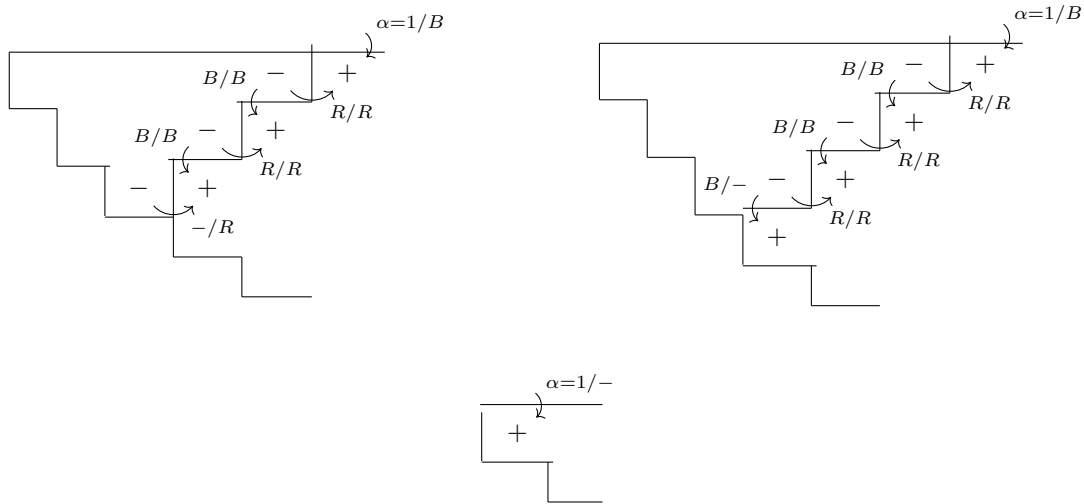


FIGURE 33. Generic insertion diagrams for the second shifted algorithm: (a) last part of  $x = 1$ , (b) last part of  $x > 1$ , and (c)  $x = \emptyset$ , which is a special case of (b)

- (1) A number being inserted into the  $P$  is inserted into the first row, with any (larger) number that it bumps being inserted into the second row, etc. as for row insertion into unshifted tableaux.
- (2) However, if a number is inserted into the main diagonal cell of a row and bumps a number, that larger number begins sequence of column insertions, starting with the first column rightward of the diagonal cell, continuing rightward until an insertion is done into an empty cell.

This insertion algorithm can be summarized straightforwardly in the insertion diagrams shown in figure 33. The diagrams show directly that the insertion algorithm is invertible and that 2 is satisfied for  $r = 1$ .

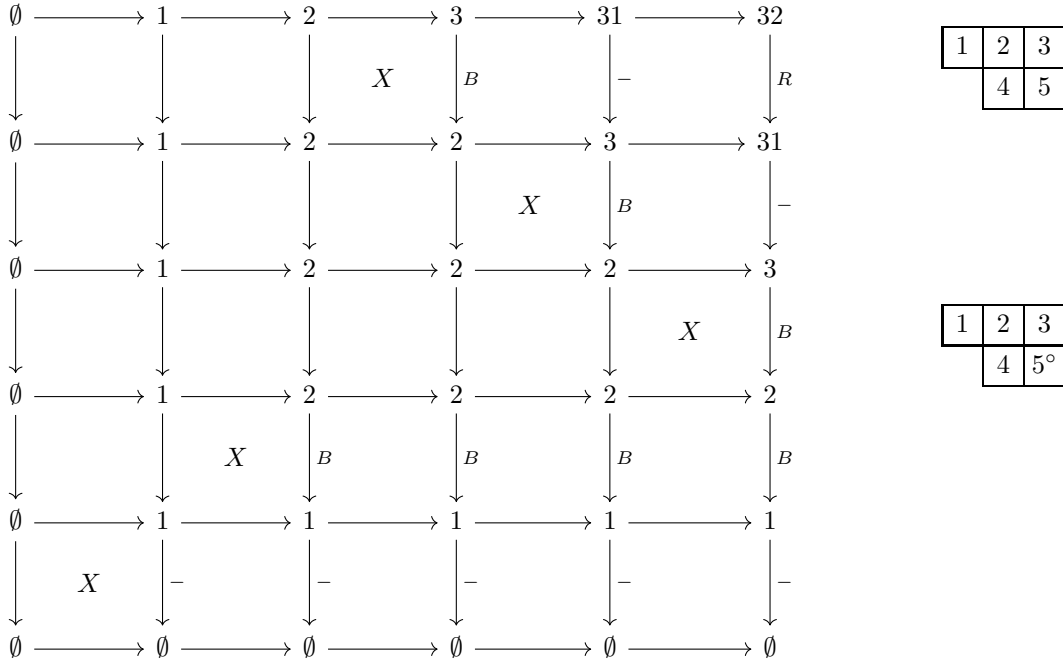


FIGURE 34. Growth for the permutation  $(1, 2, 5, 4, 3)$  for the second shifted algorithm: (a) growth diagram, (b)  $P$  tableau, and (c)  $Q$  tableau

The growth for the example permutation  $(1, 2, 5, 4, 3)$  and the resulting tableaux are shown in figure 34. Note that the only difference between the growth diagram figure 34 and the growth diagram for that permutation using the first algorithm figure 32 is the northeasternmost node, which is 32 rather than 41.

### 7. BIWEIGHTED ALGORITHMS

We can extend the weight function  $w$  and the construction of the ascending and descending graphs  $G_1$  and  $G_2$  by allowing multiple edges in  $G_1$  as well as  $G_2$ . Thus, in “biweighting”, we have two weight functions  $w_1, w_2 : B \rightarrow \mathbb{P}$ , and, as before, a differential degree  $r \in \mathbb{P}$ . Maintaining the properties of the  $U$  and  $D$  operators in [Fom1994, sec. 2.2] so as to preserve the enumerative properties of the machinery requires:

$$(12) \quad \sum_{\substack{y \in V \\ y < x}} w_1(x - y)w_2(x - y) + r = \sum_{\substack{z \in V \\ x < z}} w_1(z - x)w_2(x - y) \text{ for all } x \in V$$

Thus, from any valid biweight functions, we can construct a valid weight  $w(p) = w_1(p)w_2(p)$  and any valid weight function can be factored into valid biweight functions. Similarly, any valid weight function, paired with  $w_1(p) = 1$  becomes a valid biweight.

If we use the weight functions to specify the multiplicity of edges in  $G_1$  and  $G_2$ , then this factoring is more restrictive than we might think at first. For example, the weight function for shifted tableaux 11, since it has values of 1 and 2, is difficult to factor into integral  $w_1$  and  $w_2$  that are both nontrivial and reasonably uniform over  $B$ .

The insertion diagrams for biweighted insertion algorithms are similar to those for other algorithms. The labels on the arrows now show *four* colors:  $a_1a_2/b_1b_2$  (listing the colors of the the edges of a cell labeled as shown in figure 10), with both the “before” and “after” parts giving the  $G_1$  label before the  $G_2$  label. See e.g. figure 35.

Extending coloring to  $G_1$  allows us to extend both inversion duality and transpose duality to include a systematic change to the colors of the  $G_1$  edges and the elements of  $P$  in the straightforward way.

**7.1. Haiman’s mixed insertion.** One instantiation of a biweight (that is not a weight) is Haiman’s “mixed insertion” [Haim1989, sec. 3], with  $r = 2$ ,  $w_1(p) = 2$ , and  $w_2(p) = 1$ . The elements of the generalized permutation have two colors;  $\alpha = 1$  is called uncircled and  $\alpha = 2$  is called circled. The insertion process is [Haim1989, Def. 3.1]:

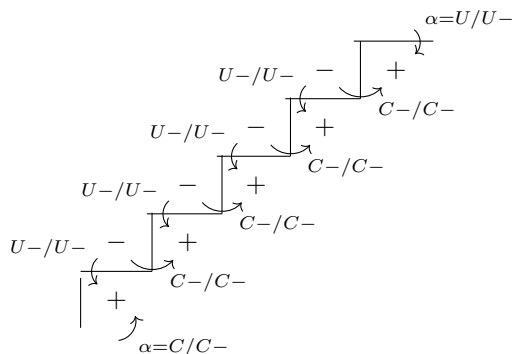


FIGURE 35. Generic insertion diagram for mixed insertion.

If  $w_i$  is not circled, insert  $w_i$  into the first row of  $T_i$ ; if it is circled, into the first column. As each subsequent element  $x$  of  $T_i$  is bumped by an insertion, insert  $x$  into the row immediately below if it is not circled, or into the column immediately to its right if it is circled. Continue until an insertion takes place at the end of a row or column, bumping no new element. As in ordinary Schensted insertion, this process terminates because (by definition) each  $x$  bumps an element greater than itself. It is easy to see that the result of the insertion process is again a tableau.

The generic insertion diagram for mixed insertion is shown in figure 35. All  $G_2$  labels are the same and are denoted “-”. Comparing figure 35 with figure 18 shows that they are inversion-duals of each other.

Because mixed insertion is the inversion-dual of left-right insertion, and left-right insertion is transpose self-dual (with interchange of “C” and “U”), mixed insertion is transpose self-dual in the same way.

An example of mixed insertion as a growth diagram is figure 36. The generalized permutation in the example is the inverse of the generalized permutation in the left-right insertion in figure 19, so the two growth diagrams are transposes of each other. Note that since  $w_2(p) = 1$ , the labels on  $G_2$  edges are not shown.

**7.2. Double-circle insertion.** Haiman remarks [Haim1989, sec. 4]

This makes it possible to define left mixed insertion, and by analogy with the definition of left-right insertion below, to define *left-right mixed insertion* (on words with two types of circles!). In such a way it is possible to get a self-dual [i.e. inversion self-dual] insertion theory that generalizes Schensted, left-right, and mixed insertion. Having no application for it in this article, we do not develop this topic here. The interested reader is invited to work out the details for him- or herself.

Here we develop this theory, not so much because we have an application for it but because using insertion diagrams, it is straightforward to decide how to define the algorithm, and using the associated software (see sec. 8) it is straightforward to execute the algorithm on permutations. Thus, we get another algorithm example with little extra work.

In order to have inversion self-duality, we require that transposition of the growth diagram creates a valid growth diagram, possibly with a systematic change of the labels on edges. This requires that both the  $G_1$  and  $G_2$  graphs have two labels on edges. Thus  $w_1(p) = 2$  and  $w_2(p) = 2$ , implying  $r = 4$ . So in regard to the biweighting, the theory is a “quadrupling” of the Robinson-Schensted theory. There are four non-zero  $\alpha$  values

- (1) represented by  $UU$  in cells and  $\cdot$  in generalized permutations
- (2) represented by  $CU$  in cells and  $\cdot^\circ$  in generalized permutations
- (3) represented by  $UC$  in cells and  $\cdot^\bullet$  in generalized permutations
- (4) represented by  $CC$  in cells and  $\cdot^\circ^\bullet$  in generalized permutations

The labels on arrows in the generic insertion diagram will be  $a_1a_2/b_1b_2$ , where each of the four elements can be “U” or “C”.

In order to have the new algorithm have the transpose self-duality of left-right and mixed insertion, that the joint transposition of the  $P$  and  $Q$  tableaux can be accomplished by changing the circling of the generalized permutation, there must be the same number of arrows “going northeast” as “going southwest” at each point in the diagram. In

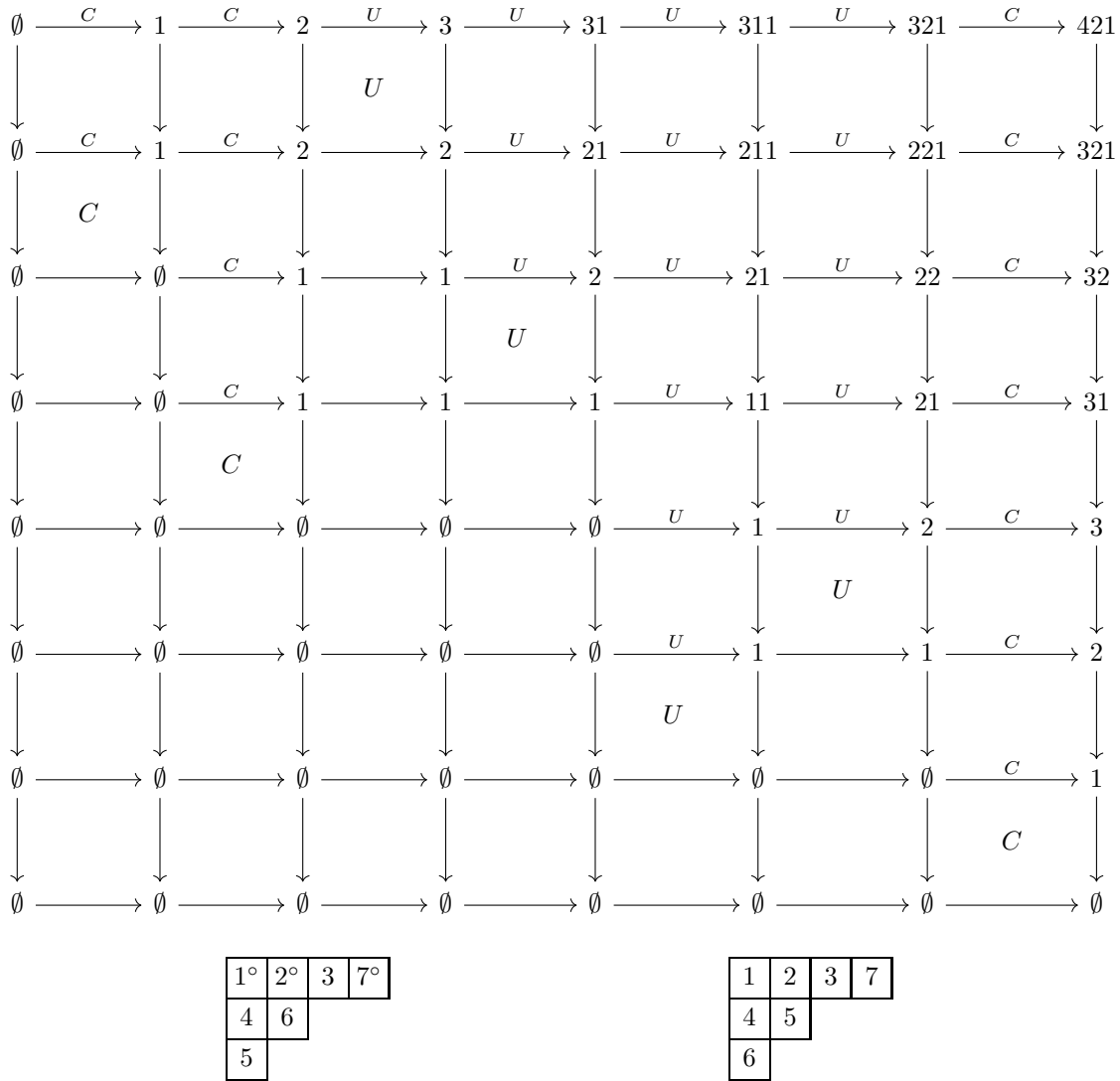


FIGURE 36. Growth for the permutation  $(7^\circ, 5, 6, 2^\circ, 4, 1^\circ, 3)$  for mixed insertion: (a) growth diagram, (b)  $P$  tableau, and (c)  $Q$  tableau

this case, each deletion point must have two arrows to the insertion point in the next row and two to the insertion point in the next column.

Similarly, each insertion point has four incoming arrows. For most insertion points, two are incoming from deletion points “from the northeast” and two from deletion points “from the southeast”. But the northeast-most insertion point has two incoming  $\alpha = \cdot$  arrows and similarly for the southwest-most insertion point. For each insertion point, one of its incoming arrows is labeled with each of the “after states”,  $UU$ ,  $UC$ ,  $CU$ , and  $CC$ .

For simplicity, and in parallel with all of the preceding unshifted insertion algorithms, each arrow has the same “before state” and “after state”. E.g. we have labels like  $UC/UC$  but not  $UC/CU$ . The result is that the arrows can be grouped into four chains, one for each circling combination, labeled with that combination as both “before state” and “after state”. Each chain begins at either the southwest or northeast extreme and passes northeastward or southwestward (resp.) through all the insertion and deletion points.

All of this reduces the number of choices to be made to  $2^4$ : For each of the chains,  $UU$ ,  $UC$ ,  $CU$ , and  $CC$ , its chain runs either southwestward or northeastward. By symmetry, one choice is arbitrary, so we choose the  $UU$  chain to run southwestward. If we choose  $UC$  or  $CU$  as the other chain running southwestward, then the other two chains



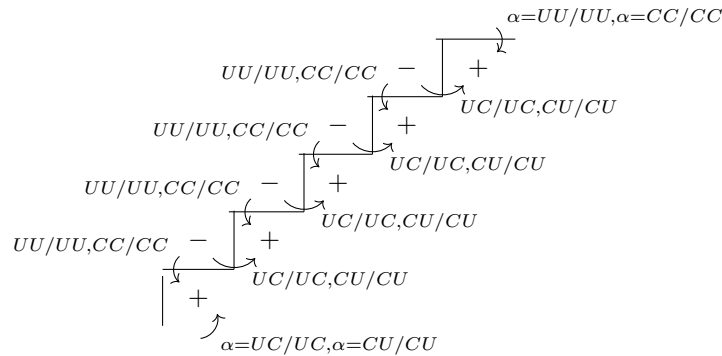


FIGURE 37. Generic insertion diagram for double-circle insertion

run northeastward, and either the first or second (resp.) circling does not affect the insertion process itself, and just passes through to label the elements in one of the result tableaux.

Thus, the only interesting choice is to have the  $UU$  and  $CC$  chains run southwestward and the  $UC$  and  $CU$  chains run northeastward. This generic insertion diagram is shown in figure 37. A typical growth diagram is shown in figure 38.

**7.3. Haiman’s shifted mixed insertion.** Haiman defines shifted mixed insertion [Haim1989, sec. 3 and Def. 6.7]

We now describe a shifted version of mixed insertion that has a symmetry relationship (Proposition 6.8) to unshifted mixed insertion parallel to the relationship between Worley-Sagan insertion and left-right insertion given by Proposition 6.2. [...]

Let  $w = w_1 \cdots w_n$ , be a word without circles. Construct a sequence  $T_0, T_1, \dots, T_n = T$  of shifted tableaux with circles: [...]

Insert  $w_i$  into the first row, and insert bumped letters as in mixed insertion: circled letters, bumped, insert into the next column; uncircled letters, into the next row, with one exception. The exception is that an uncircled letter, bumped from a diagonal cell, acquires a circle and inserts into the next column.

The generic insertion diagrams are shown in figure 39. Note that all the nontrivial labels are for  $G_1$ .

An example of the algorithm is shown in figure 40. Since the permutation  $(1, 2, 5, 4, 3)$  is its own inverse, this growth is inversion-dual to the shifted growth in figure 34. That shifted mixed insertion is inversion-dual to the second shifted insertion can be seen directly by comparing the insertion diagrams, figures 33 and 39.

**7.4. McLarnan’s shifted column insertion.** [McLar1986, sec. 3, p. 49 et seq.] defines a shifted insertion algorithm with an interesting set of properties. The insertion diagrams for the algorithm are figure 41. Expressed as an algorithm, it is straightforward: insert the number using column insertion, starting in the first column into which it can be inserted, circling the number in the  $P$  tableau if it was initially inserted into an off-diagonal cell. An example growth diagram is shown in figure 42.

McLarnan constructed the algorithm to be “symmetric”, that is as close as possible to being inversion self-dual. Inversion self-duality can’t be achieved, because shifted tableau do not admit the weight  $w(x) = 1$  and so the multiplicity of the  $G_1$  edges and  $G_2$  edges cannot be the same. This prevents the  $P$  and  $Q$  tableau from being interchanged in the strict sense. This is apparent in the generic insertion diagrams and the example growth diagram.

However, inverting the permutation does swap the  $P$  and  $Q$  tableaux as long as the circling is ignored. Moreover, the circles in the permutation’s  $P$  tableau are effectively moved to the elements in the inverse’s  $P$  tableau (the permutation’s  $Q$  tableau) that are the corresponding elements in the inverse permutation. For example, the inverse of the permutation in figure 42 is shown in figure 43.

McLarnan arranged for this inversion near-duality by arranging that the movement of an element upon bumping is not dependent on its circled status. In the context of a growth diagram, the labels on the  $G_1$  edges pass northward through the diagram, neither being changed by more northern cells nor affecting the nodes of more northern cells.

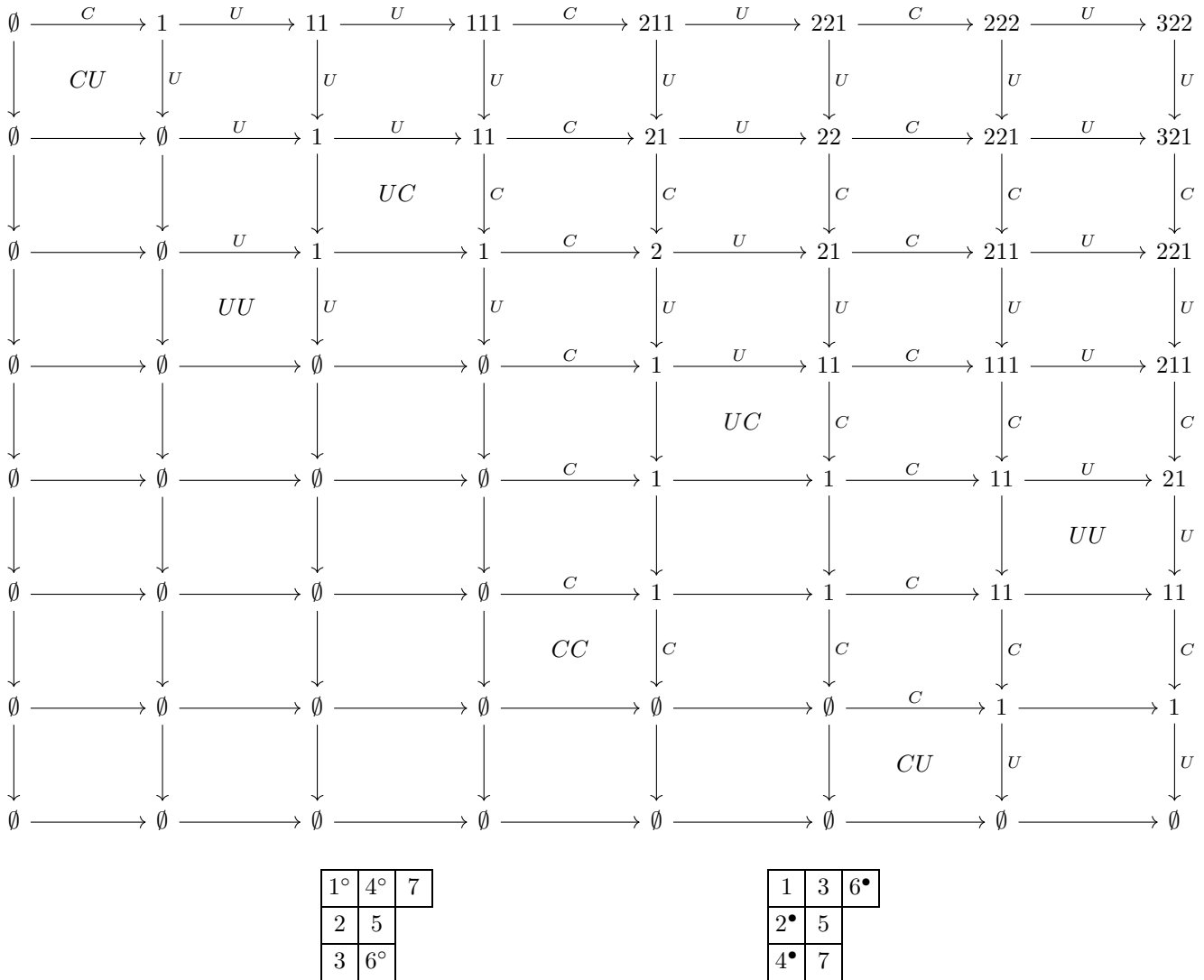


FIGURE 38. Growth for double-circle for the permutation  $(6^\circ, 4^\circ, 7, 5^\bullet, 2, 3^\bullet, 1^\circ)$

**7.5. Dual shifted column insertion.** For our purposes, the inversion-dual of the shifted column algorithm, which we call *dual shifted column insertion*, is more interesting. Indeed, we believe that it deserves more study in the theory of tableau insertion algorithms than it has received.

Because shifted column insertion is nearly inversion self-dual, the only difference from shifted column insertion is that labels are attached to the  $G_2$  edges rather than the  $G_1$  edges, and so circles appear on the elements of the  $Q$  tableau. See figure 44 for the generic insertion diagrams, and figure 45 for an example growth diagram.

This algorithm is close in style to the first 6.1 and second 6.2 shifted algorithms. It is simpler and more intuitive than either of them, and is nearly inversion self-dual (in the same way as shifted column insertion). And since it only applies labels to  $G_2$  edges, it is compatible with the original formulation of growth diagrams 2.7.

It is a matter of interest why such a straightforward variant of a described algorithm has apparently not been described before now. That appears to be due to the general neglect of McLarnan's shifted column insertion. One driver of that may be that because shifted column insertion puts circles on elements of  $P$  rather than  $Q$  it is less congruent with other early algorithms for shifted tableaux, which put circles only on elements of  $Q$ , and consequently it is not compatible with the original formulation of growth diagrams. Putting circles on elements of  $P$  is natural in McLarnan's approach, but not so putting circles on elements of  $Q$ .

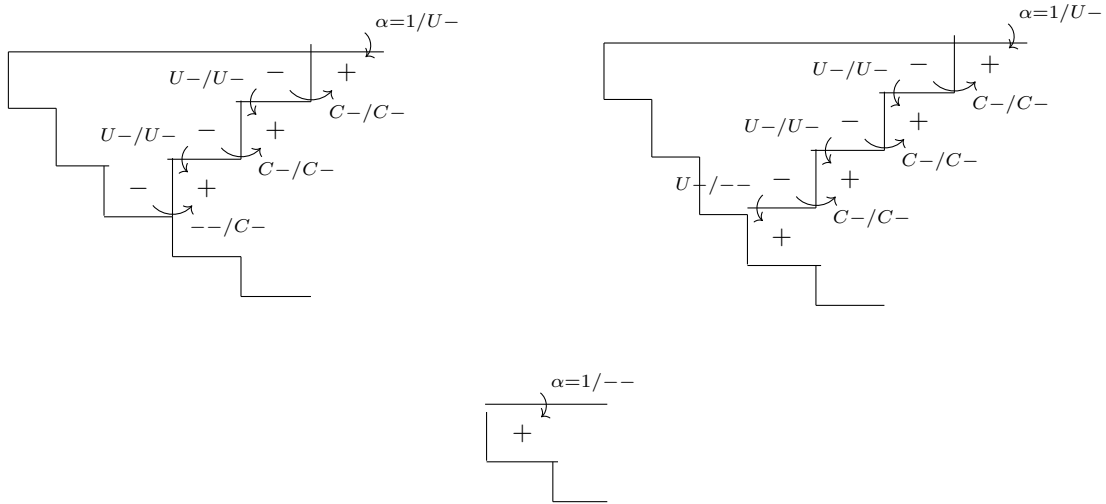


FIGURE 39. Generic insertion diagrams for shifted mixed insertion

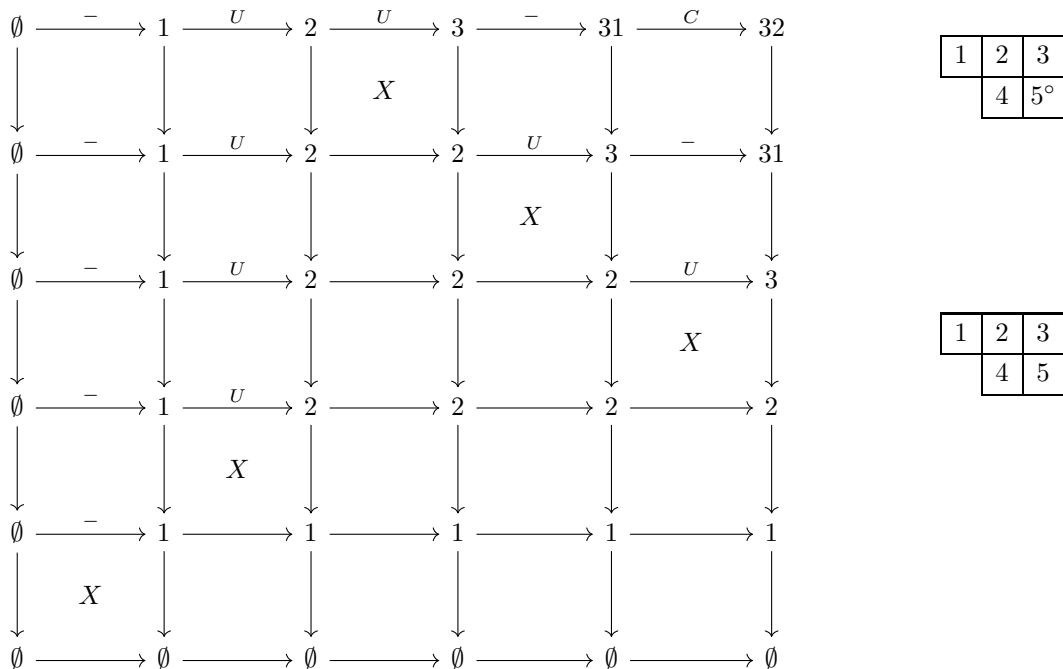


FIGURE 40. Growth for the permutation  $(1, 2, 5, 4, 3)$  for the shifted mixed insertion: (a) growth diagram, (b)  $P$  tableau, and (c)  $Q$  tableau. This is inversion-dual to  $34$  because the permutation is an involution.

Early work on other shifted algorithms tended to put circles on elements of  $Q$  as that allowed circles on elements of the generalized permutation, which then propagate to the elements of  $P$ .

Conversely, Sagan’s approaches via the Knuth relations [Sag1979] and the “lifting” operation [Sag1987] and Worley’s approach via jeu de taquin [Wor1984] do not seem to naturally lead to this algorithm.

Another factor is likely that Sagan and Worley both started searching for algorithms based on row insertion, as that is the most commonly-used unshifted algorithm, and both succeeded at that. Neither seems to have considered

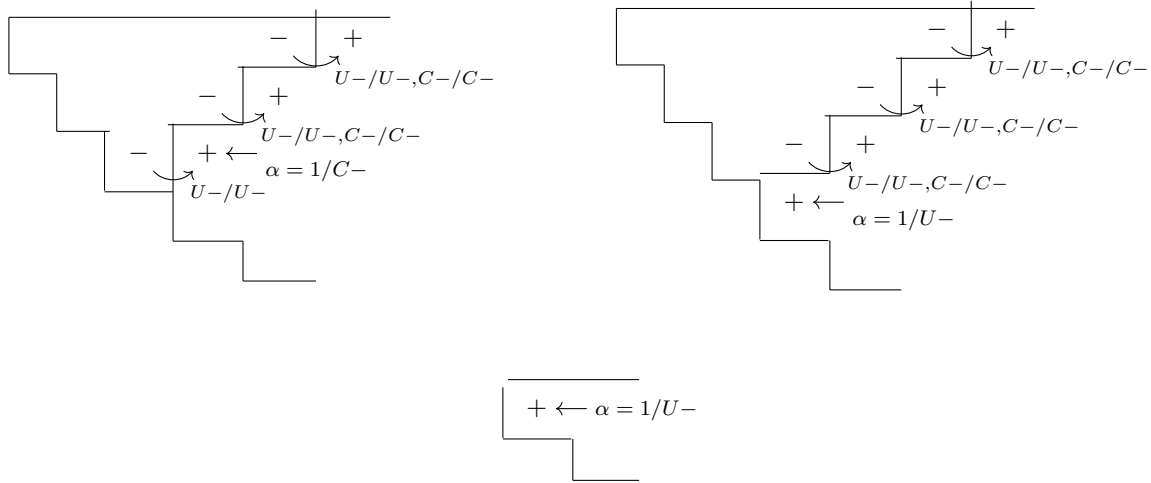


FIGURE 41. Generic insertion diagrams for shifted column insertion

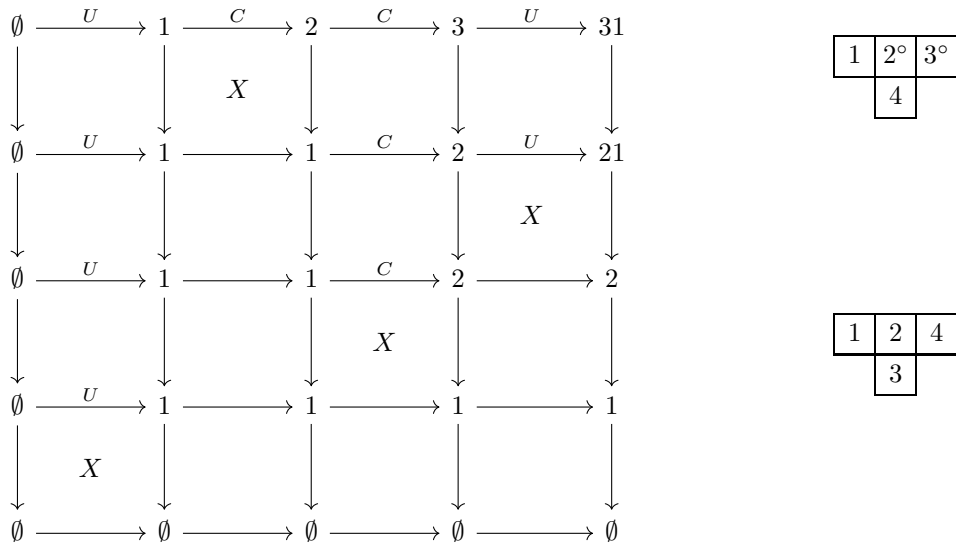


FIGURE 42. Growth for the permutation  $(1, 3, 4, 2)$  for McLarnan's shifted column insertion: (a) growth diagram, (b)  $P$  tableau, and (c)  $Q$  tableau

starting with column insertion. In the context of unshifted tableaux, row and column insertion are simply transpose-dual, which suggests that attacking the problem of shifted tableaux starting with either row or column insertion will give the same results. But with shifted tableaux row and column insertion are distinctly different.

### 8. SOFTWARE

There are two ancillary software files:

**growth.py** – (Python) A large number of classes containing machinery for executing tableau insertion algorithms.

**growth-driver.py** – (Python) A driver program that uses the machinery in **growth.py** for several dozen tests/examples, including many examples in this paper.

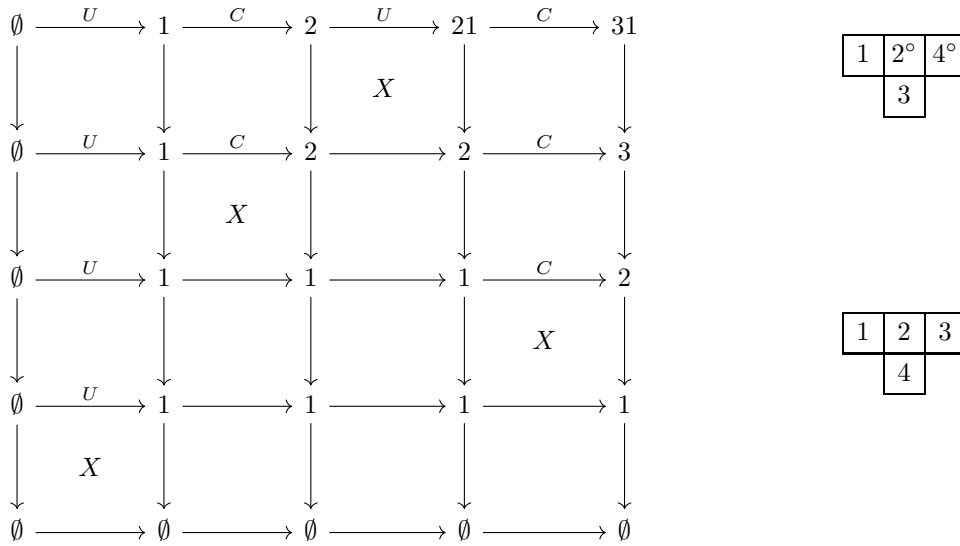


FIGURE 43. Growth for the permutation  $(1, 4, 2, 3)$  for McLarnan's shifted column insertion, which is the inverse of the permutation in 42

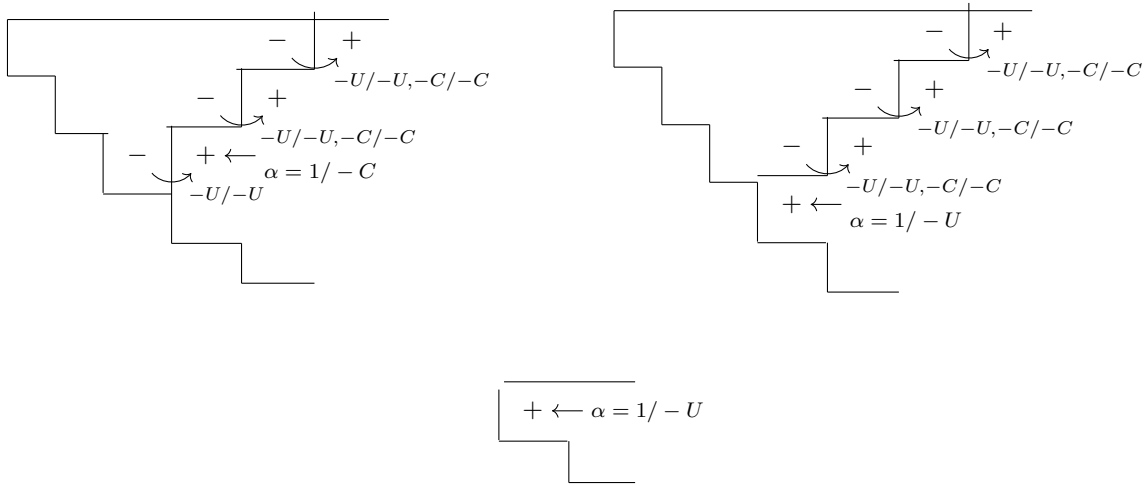


FIGURE 44. Generic insertion diagram for dual shifted column insertion

9. REFERENCES

[Fom1994] Sergey Fomin, *Duality of Graded Graphs*, Journal of Algebraic Combinatorics **3** (1994), 357–404, DOI 10.1023/A:1022412010826, available at <https://link.springer.com/content/pdf/10.1023/A:1022412010826.pdf>.  
<https://scholar.google.com/scholar?cluster=3401296478290474488>.

[Fom1995] ———, *Schensted Algorithms for Dual Graded Graphs*, Journal of Algebraic Combinatorics **4** (1995), 5–45, DOI 10.1023/A:1022404807578, available at <https://link.springer.com/content/pdf/10.1023/A:1022404807578.pdf>.  
<https://scholar.google.com/scholar?cluster=9003315695694762360>.

[GarMcLar1987] Adriano M. Garsia and Timothy J. McLarnan, *Robinson-Schensted Algorithms Obtained from Tableau Recursions* (1987), arXiv 2201.12908, primary class math.CO,

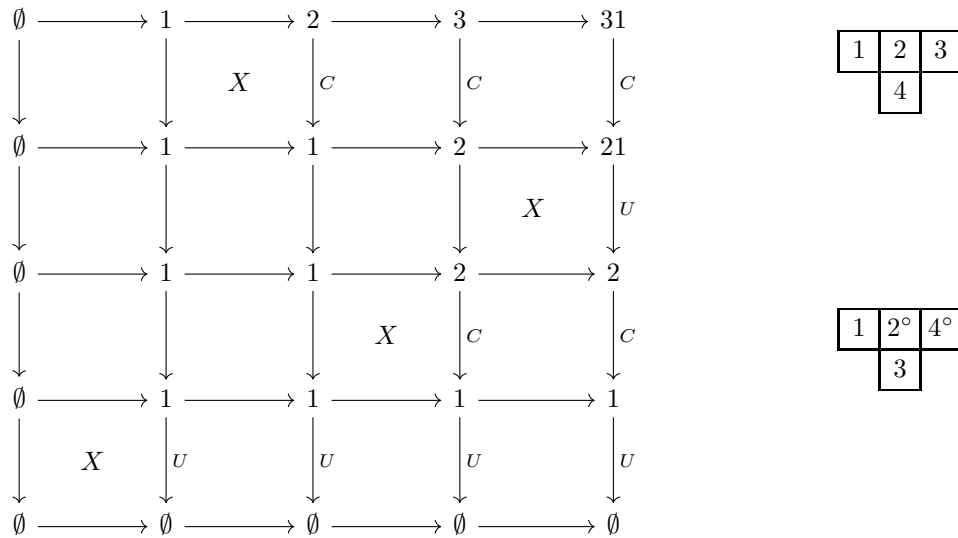


FIGURE 45. Growth for the permutation  $(1, 3, 4, 2)$  for dual shifted column insertion: (a) growth diagram, (b)  $P$  tableau, and (c)  $Q$  tableau

- DOI 10.48550/arXiv.2201.12908, available at <https://arxiv.org/abs/2201.12908>.  
<https://scholar.google.com/scholar?cluster=446442338380191517>
- [Haim1989] Mark D. Haiman, *On mixed insertion, symmetry, and shifted Young tableaux*, J. Combin. Theory **Ser. A** **50** (1989), 196–225, DOI 10.1016/0097-3165(89)90015-0, available at <https://www.sciencedirect.com/science/article/pii/0097316589900150>.  
<https://scholar.google.com/scholar?cluster=14350300647709625382>.
- [Lam2008] Thomas F. Lam, *Signed differential posets and sign-imbalance*, J. Combin. Theory **Ser. A** **115** (2008), 466–484, DOI 10.1016/j.jcta.2007.07.003, available at <https://www.sciencedirect.com/science/article/pii/S0097316507000957>.  
<https://scholar.google.com/scholar?cluster=7312628064545996659>.
- [McLar1986] Timothy J. McLarnan, *Tableau Recursions and Symmetric Schensted Correspondences for Ordinary, Shifted and Oscillating Tableaux*, Ph.D. Thesis, U. C. San Diego, 1986.  
<https://scholar.google.com/scholar?cluster=6563465974933598796>.
- [Mooers1959] Calvin N. Mooers, *The Next Twenty Years in Information Retrieval: Some Goals and Predictions*, Proceedings of the Western Joint Computer Conference (San Francisco, 1959), pp. 81–86, DOI 10.1145/1457838.1457853, available at <https://dl.acm.org/doi/pdf/10.1145/1457838.1457853>.  
<https://scholar.google.com/scholar?cluster=6065334782042092209>.
- [Roby1991] Tom W. Roby, *Applications and extensions of Fomin's generalization of the Robinson-Schensted correspondence to differential posets*, Ph.D. Thesis, Massachusetts Institute of Technology, 1991, <https://dspace.mit.edu/bitstream/handle/1721.1/13517/25933623-MIT.pdf>.  
<https://scholar.google.com/scholar?cluster=9893116474914970883>.
- [Sag1979] Bruce Sagan, *An analog of Schensted's algorithm for shifted Young tableaux*, J. Combin. Theory **Ser. A** **27** (1979), 10–18, DOI 10.1016/B978-0-12-428780-8.50007-6, available at <https://users.math.msu.edu/users/bsagan/Papers/Old/asa-pub.pdf>.  
<https://scholar.google.com/scholar?cluster=15694654829594027728>. MR80k 05029
- [Sag1987] ———, *Shifted tableaux, Schur  $Q$ -functions, and a conjecture of R. P. Stanley*, J. Combin. Theory **Ser. A** **45** (1987), 62–103, DOI 10.1016/0097-3165(87)90047-1, available at <https://users.math.msu.edu/users/bsagan/Papers/Old/sts-pub.pdf>.  
<https://scholar.google.com/scholar?cluster=17936398118720156955>.

- [Schen1961] Craig Schensted, *Longest increasing and decreasing sequences*, *Canad. J. Math.* **13** (1961), 179–191, DOI 10.4153/CJM-1961-015-3, available at <https://www.cambridge.org/core/services/aop-cambridge-core/content/view/B5098D9BC8B226C57540>
- [Stan1988] Richard P. Stanley, *Differential Posets*, *J. Amer. Math. Soc.* **1** (1988), 919–961, DOI 10.2307/1990995, available at <https://www.jstor.org/stable/1990995>.  
<https://scholar.google.com/scholar?cluster=5318386056862341375>.
- [Stan1990] ———, *Variations on differential posets*, *Invariant Theory and Tableaux* (Dennis Stanton, ed.), *IMA Volumes in Math. and Its Appls.*, vol. 19, Springer-Verlag, Berlin and New York, 1990, 1990, pp. 145–165, available at <https://math.mit.edu/~rstan/pubs/pubfiles/78.pdf>.  
<https://scholar.google.com/scholar?cluster=2941535162033905939>.
- [Stan2012] ———, *Enumerative Combinatorics, Volume 1*, 2nd ed., *Cambridge Studies in Advanced Mathematics*, vol. 49, Cambridge University Press, Cambridge, 1997, 2012. original edition 1997.
- [Wor1984] Dale R. Worley, *A Theory of Shifted Young Tableaux*, Ph.D. Thesis, Massachusetts Institute of Technology, 1984. <https://scholar.google.com/scholar?cluster=7106851617217394040>.

*Email address:* worley@alum.mit.edu